3-Hydroxypyridin-2-thione as Novel Zinc Binding Group for Selective Histone Deacetylase Inhibition

Vishal Patil,[†,||] Quaovi H. Sodji,[†,||] James R. Kornacki,[§] Milan Mrksich,*[,§] and Adegboyega K. Oyelere*[,†,‡]

[†]School of Chemistry and Biochemistry, [‡]Parker H. Petit Institute for Bioengineering and Bioscience, Georgia Institute of Technology, Atlanta, Georgia 30332-0400, United States

[§]Department of Chemistry and Howard Hughes Medical Institute, Northwestern University, 2145 Sheridan Road, Evanston, Illinois 60208-3113, United States

S *Supporting Information*

ABSTRACT: Small molecules bearing hydroxamic acid as the zinc binding group (ZBG) have been the most effective histone deacetylase inhibitors (HDACi) to date. However, concerns about the pharmacokinetic liabilities of the hydroxamic acid moiety have stimulated research efforts aimed at finding alternative nonhydroxamate ZBGs. We have identified 3-hydroxypyridin-2-thione (3-HPT) as a novel ZBG that is compatible with HDAC inhibition. 3-HPT inhibits HDAC 6 and HDAC 8 with an IC_{50} of 681 and 3675 nM, respectively. Remarkably, 3-HPT gives no inhibition of HDAC 1. Subsequent optimization led to several novel 3HPT-based HDACi that are selective for HDAC 6 and HDAC 8. Furthermore, a subset of these inhibitors induces apoptosis in various cancer cell lines.
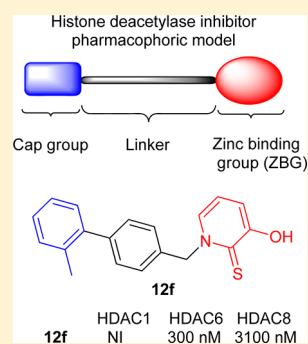
INTRODUCTION

Eukaryotic DNA is wrapped around nucleosomes comprised of histone proteins that are subjected to various post-translational modifications including acetylation, phosphorylation, sumoylation, and methylation. These post-translational modifications function to regulate transcription.[1,2] Histone acetylation/deactylation, which have been the most studied covalent modifications, are mediated by the histone acetyl transferases (HATs) and the histone deacetylases (HDACs), respectively.[3,4] We now know that a significant fraction of cellular proteins are also substrates for HDAC and HAT enzymes, extending their role beyond that of transcriptional regulation.[5] Presumably due to their involvement in repressing transcription, various HDAC isoforms are overexpressed in different cancers and as such are valid targets for cancer treatment.[6] In fact, two histone deacetylase inhibitors (HDACi), suberoylanilide hydroxamic acid (SAHA) and cyclic peptide FK228, are approved for the treatment of cutaneous T-cell lymphoma (CTCL).[4] Other pathological conditions where targeting HDAC constitute a plausible therapeutic option include inflammatory diseases, parasitic infections, hemoglobinopathies, and neurodegenerative diseases.[7−10]

The classic pharmacophoric model of HDACi consists of a zinc binding group (ZBG) that chelates the active site Zn^{2+} ion, a linker, and a surface recognition cap group that interacts with the amino acid residues present at the surface of the HDAC (Figure 1).[11]

Chelation of the Zn^{2+} ion has proven crucial for HDAC inhibition.[12] The hydroxamic acid has been the preferred ZBG due to its strong Zn^{2+} ion chelation.[13,14] Yet the hydroxamic acid could present metabolic and pharmacokinetic challenges,

including a short half-life and poor bioavailability.[15−17] The hydroxamate also chelates other biologically relevant metals, including Fe^{2+} and Cu^{2+}, with affinities that can exceed that of Zn^{2+} ion.[18,19] Extensive reports have aimed to improve the HDAC inhibition profile by manipulating the surface recognition cap group and linker region while retaining the hydroxamic acid as ZBG. Indeed, these efforts have resulted in highly potent and, in some cases, isoform-selective compounds.[20,21]

Several efforts have replaced the hydroxamic acid with alternative chemical moieties.[22] For example, MS-275 is a class I selective HDACi having a benzamide ZBG.[23] It has been suggested that the benzamide ZBG exploits the difference in the region adjacent to the active site to achieve its isoform selectivity.[24] Further, subtle differences in the active sites of various HDAC isoforms have been exploited to design compounds having other ZBGs, including thiols, α-ketoesters, electrophilic ketones, mercaptoamides, and phosphonates.[11,25] However, most of these analogues had reduced potency.

Nonhydroxamate chemotypes that chelate Zn^{2+} ion have been well studied in the context of inhibitors of the matrix metalloproteins (MMPs) (Figure 2). This work has revealed that bidentate heterocyclic ZBGs are stronger metal chelators than are the monodentate analogues.[26,27] Furthermore, the bidentate heterocyclic ZBGs are resistant to hydrolysis and are effective at inhibiting the proteinase activities of various MMP isoforms.[27] We therefore borrowed the bidentate heterocyclic ZBGs to evaluate a new class of HDACi that may be devoid of
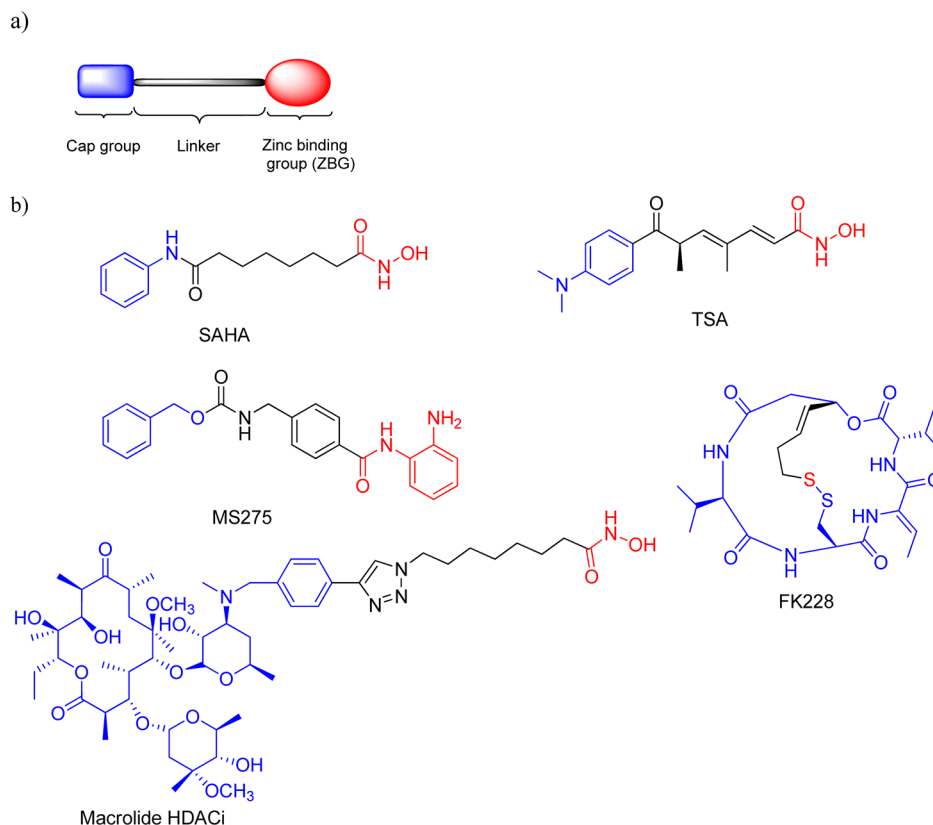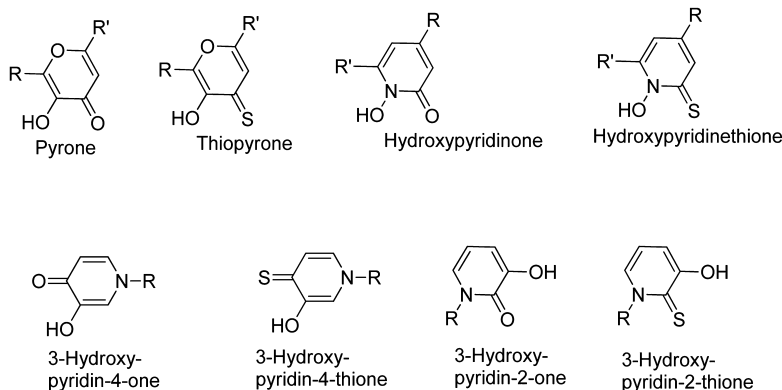
Figure 1. (a) HDACi pharmacophoric model. (b) Representative examples of HDACi (note color code highlights the three pharmacophores).
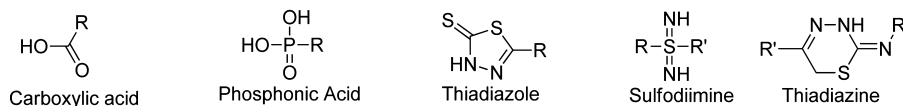

Figure 2. Representative examples of bidentate heterocyclic and monodentate nonhydroxamate ZBGs.[26,28]

many of the liabilities of the hydroxamate moiety. We herein report that 3-hydroxypyridin-2-thione (3-HPT) is a bidentate heterocyclic ZBG that is compatible with HDAC inhibition. 3-HPT inhibits the deacetylase activities of HDAC 6 and HDAC 8 with IC_{50} of 680 and 3700 nM, respectively. Remarkably, 3-HPT is inactive against HDAC 1. Subsequent optimization led to several novel 3-HPT-based HDACi that are selective for

HDAC 6 and HDAC 8. Furthermore, a subset of these inhibitors induces apoptosis in various cancer cell lines.

■ **RESULTS AND DISCUSSION**

Initial Molecular Docking Studies. We first performed molecular docking analyses on selected bidentate heterocyclic ZBG fragments against three HDAC isoforms: HDAC 1,

HDAC 6, and HDAC 8. Our choice of bidendate ZBG fragments is informed by their reported Zn^{2+} ion chelation affinity and the ease with which subsequent modification could be introduced to enhance potency.[26,27] The bidendate ZBG fragments that met these criteria, 3-hydroxypyridin-2-one, 3-hydroxypyridin-2-thione, 3-hydroxypyridin-4-thione, and 1-hydroxypyridin-2-thione, were selected for initial studies (Figure 3). We performed docking analyses against the crystal
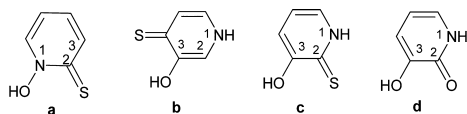

Figure 3. Docked bidendate ZBG fragments: (a) 1-hydroxypyridin-2-thione (**1a**), (b) 3-hydroxypyridin-4-thione (**1b**), (c) 3-hydroxypyridin-2-thione (3-HPT) (**2**), (d) 3-hydroxypyridin-2-one (3-HP) (**3**).

structures of HDAC 8 (PDB code: 1VKG),[29] histone deacetylase-like protein (HDLP), a HDAC 1 homologue,[12] and the homology models of HDAC 1 and HDAC 6 built respectively from human HDAC 2 (PDB code: 3MAX) and HDAC 8 (PDB code: 3FOR)[21] using a validated molecular docking program (AutoDock 4.2) as described previously.[30,31]

Preliminary docking analyses revealed that 3-hydroxypyridin-2-one (3-HP), 3-hydroxypyridin-2-thione (3-HPT), 3-hydroxypyridin-4-thione, and 1-hydroxypyridin-2-thione chelate the Zn^{2+} ion at active site of HDLP, HDACs 1, 6 and 8, suggesting that these bidendate heterocycles could provide the critical ZBG in the HDACi pharmacophoric model. A closer inspection of the docked poses in HDACs 1, 6, and 8 revealed that the N-1 position of 3-hydroxypyridin-4-thione is oriented toward the base of the active site pocket as opposed to the N-1 positions of 3-HP and 3-HPT, which are oriented toward the surface of the channel that the linker region of prototypical HDACi occupies to present the surface recognition cap group to the enzyme outer rim. Conversely, the docked poses of 3-HP and 3-HPT at HDLP active site that retained zinc chelation are those in which their N1-positions are oriented toward the base of the active site pocket in similar manner to the N-1 position of 3-hydroxypyridin-4-thione (Supporting Information, Figures S1–S3). In HDLP, the N-1 position of 3-HPT engages in hydrogen bonding with GLY129, which stabilizes its orientation, however, in the HDAC 1 homology model, the outward orientation of the 3-HPT is probably influenced by the prospect of hydrogen bonding of its N-1 with TYR303 phenol group and GLY149 backbone (Supporting Information, Figure S1C).

The docked poses adopted by 3-HP and 3-HPT, particularly on HDACs 6 and 8, should enable facile introduction of linkers and surface recognition cap groups through the N-1 position in order to further enhance HDAC inhibition potency. Such modifications, however, could compromise inhibition activity of the 3-hydroxypyridin-4-thione fragment as its N-1 position

participates in potentially stabilizing H-bonding interactions at the base of the enzyme active sites. Although 1-hydroxypyridin-2-thione shows Zn^{2+} ion chelation at HDAC active sites (Supporting Information, Figures S1–S3), this ZBG is similar to hydroxamic acid and it is synthetically less tractable relative to 3-HP and 3-HPT. On the basis of these observations, we directed our efforts on the 3-HP and 3-HPT fragments. To test the validity of our in silico predictions, we investigated the effects of 3-HPT **2** and 3-HP **3** on the deacetylase activities of HDAC 1, HDAC 6, and HDAC 8. 3-HPT **2** was synthesized from the commercially available 3-hydroxypyridin-2-one as previously reported.[32]
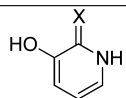
In Vitro HDAC Inhibition Activity of 3-HP and 3-HPT Fragments. We used SAMDI mass spectrometry as previously described to assay inhibitor potency against the HDAC isoforms 1, 6, and 8.[30,33,34] 3-HPT **2** inhibited HDAC6 with an IC_{50} of 680 nM and inhibited HDAC8 with an IC_{50} of 3.7 μM. This compound had no activity against HDAC 1 (Table 1). The analogue 3-HP **3** was inactive against each of the three HDAC isoforms. The disparity in the HDAC inhibition activity of 3-HP and 3-HPT could be due to the thiophilicity of zinc which favors 3-HPT.[35]

The inactivity of 3-HPT against HDAC 1 may not be surprising giving the ambivalence of its interaction with the HDAC 1 (homology model) and HDLP active sites (Supporting Information, Figure S1). This data suggests that the docked structure of 3-HPT on HDLP may closely mimic its binding with HDAC 1. Alternatively, it is plausible that the narrowness of HDAC 1 tunnel, relative to those of HDAC 6 and HDAC 8, could constitute a challenge toward proper accommodation of 3-HPT at HDAC 1 active site. HDAC 1 activity or lack thereof could then be influenced by conformational changes which are not captured by docking analysis such as AutoDock.

Structure–Activity Relationship (SAR) Studies. We next performed docking analyses of the N-1 methyl, benzyl, and biphenyl derivatives of 3-HP and 3-HPT and found that the compounds were predicted by AutoDock to adopt docking poses similar to 3-HP and 3-HPT (see Supporting Information Figures S4 and S5 for docking results on N-1 methyl derivative). We then synthesized representative examples of these compounds, N-1 methyl (**5a**), benzyl (**5b** and **7b**), and biphenyl (**5c** and **7c**) derivatives (Scheme 1), and tested their HDAC inhibition activities against HDACs 1, 6, and 8. As observed with the 3-HP/3-HPT pair, carbonyl-compounds **5a**, **5b**, and **5c** failed to inhibit HDAC activity (data not shown). The thione-compounds **7b** and **7c** inhibited HDAC 6 with midnanomolar IC_{50}s and less potent activity against HDAC 8 (Table 2). Similar to our observation with 3-HPT, neither **7b** nor **7c** possess any measurable activity against HDAC 1 at maximum tested concentration of 10 μM. The anti-HDAC 6 and 8 activities of **7b** and **7c** mirrored those of 3-HPT,

Table 1. HDAC Inhibition Activities of 3-HP and 3-HPT[a]

Compound	X	HDAC1 IC_{50} (nM)	HDAC6 IC_{50} (nM)	HDAC8 IC_{50} (nM)
	O	NI†	NI	NI
	S	NI	681 ± 110	3675 ± 1201

[a]Activities determined by SAMDI analysis. †No significant Inhibition (below 20% Inhibition) at maximum tested concentration of 10 μM.

Scheme 1. Synthesis of the 3-HP and 3HPT-Based ZBG HDACi[a]
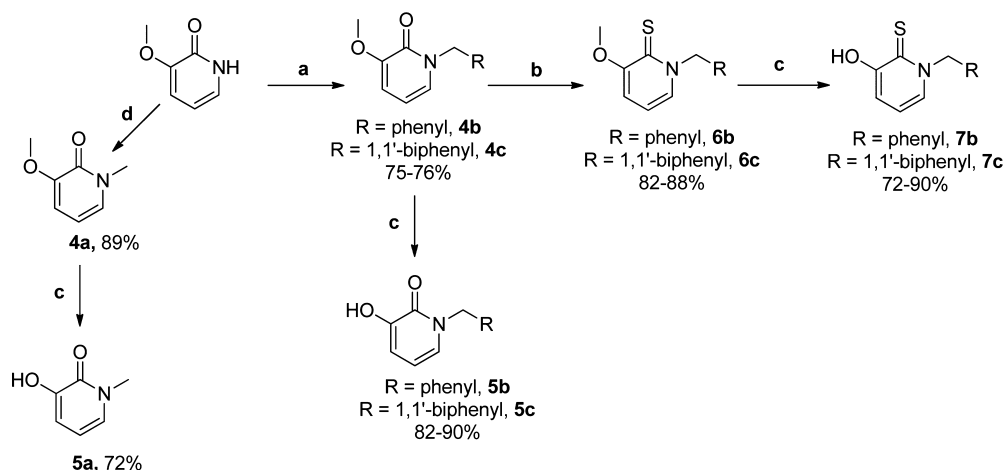
[a] (a) R-CH$_2$Br, K$_2$CO$_3$, DMF, 100 °C; (b) Lawesson's reagent, toluene, reflux; (c) BBr$_3$, CH$_2$Cl$_2$; (d) MeI, KOH, MeOH, rt.

however, **7b** is somewhat more active against both HDAC isoforms. That the biphenyl moiety of **7c** did not increase affinity of this compound for the HDAC may reflect a lack of interactions of this hydrophobic group with the hydrogen-bonding surface of the protein channel.

We reasoned that the diaryl moiety of **7c** could be tuned to introduce interactions with the enzyme active site channel residues. We substituted the proximal phenyl group with a 1,2,3-triazole ring to give analogues **15a** and **17a**. In silico interrogation against HDACs 6 and 8 again revealed that **15a** and **17a** adopted poses whereby the active site Zn^{2+} ion chelation is maintained in both isoforms. Interestingly, the triazole ring of either compound is positioned close to the HDAC 8 Tyr306 OH-group for possible H-bonding. The analogous interaction is missing in HDAC 6 (Figure 4; note that only the docked poses of the 3-HPT diaryl **17a** are shown for clarity).

We next synthesized the diaryl compounds **15a** and **17a** and their analogues (discussed later) using the route shown in Scheme 3 and tested their HDAC inhibition activities against HDACs 1, 6, and 8. Consistent with the observations described above, the 3-HP compound **15a** is inactive against the HDAC isoforms tested. Surprisingly, 3-HPT diaryl **17a** is only marginally inhibitory to HDAC 6 at a concentration of 10 μM, quite in contrast to the effect of the analogous compound **7c**. We also found that **17a** is about 2−3-fold more active against HDAC 8 relative to **7c** (Table 2). This result is consistent with our in silico observation which suggested that the triazole ring could be beneficial to HDAC 8 inhibition (Figure 4).

Encouraged by these results, we focused our SAR studies on **7c** and **17a** as leads, introducing substituents at the distal phenyl group (relative to the ZBG). We prepared a series of aromatic and heteroaromatic derivatives to investigate the effect of the substitution pattern and the nature of substituents on inhibition activity. Because we used a Suzuki cross coupling[36] to join the 3-HP phenyl bromide **8** with a phenyl boronic acid, we could readily prepare several analogous biphenyl compounds (**9a−i**). Subsequent deprotection of the *O*-methoxy group with boron tribromide gave 3-HP biphenyl compounds **11a−i**. Alternatively, the reaction of **9a−i** with Lawesson's reagent resulted in *O*-methoxy protected 3-HPT biphenyl compounds

10a−i, which upon treatment with boron tribromide furnished the desired 3-HPT biphenyl compounds **12a−i** (Scheme 2).

Consistent with the pattern seen with the previous analogues, all 3-HP biphenyl compounds **11a−i** lacked HDAC inhibition activity against HDACs 1, 6, and 8 (data not shown). Similarly, all the 3-HPT biphenyl compounds **12a−i** are inactive against HDAC 1 while the majority possess substituent dependent inhibitory activities against HDACs 6 and 8 with varying degrees of selectivity for either isoform (Table 2). Compound **12a**, an analogue of **7c** with a cyano-substituent at the *para*-position, inhibits HDAC 6 at a level nearly identical to that of **7c** while it is about 2-fold better HDAC 8 inhibitor relative to **7c**. A shift of the cyano-substitution to the *meta*-position in compound **12b** resulted in the abrogation of HDAC 6 inhibition while a slight enhancement of HDAC 8 inhibition was observed. *Ortho* placement of the cyano-substituent in compound **12c** restored HDAC 6 inhibition with higher potency relative to compounds **7b** and **7c**, while HDAC 8 inhibitory activity remained largely unperturbed. Interestingly, methyl substituted compounds **12d−f** are strongly inhibitory to HDAC 6 irrespective of the position of substitution. In fact, compound **12f** is the strongest HDAC 6 inhibitor in this series of 3-HPT biphenyl compounds with IC$_{50}$ of 306 nM (Table 2). Conversely, the ability of compounds **12d−f** to inhibit HDAC 8 is very sensitive to the placement of the methyl substituent. The *para*-methyl derivative **12d** is more active, with IC$_{50}$ of 800 nM, than the corresponding *meta*-methyl and *ortho*-methyl analogues, **12e** and **12f**, respectively. Placement of the electron donating *N,N*-dimethylamino group at the *para*-position in compound **12g**, analogous to the substitution pattern on the surface recognition group of simple HDACi Trichostatin A (TSA), resulted in loss of HDAC 6 inhibition while HDAC 8 inhibition activity at micromolar IC$_{50}$ is about 2-fold enhanced relative to the lead compound **7c**. The 4-pyridyl substitution in compound **12i** partially restored HDAC 6 inhibition lost in **12g** without any added benefit to HDAC 8 inhibition. Interestingly, the combination of pyridine and *N,N*-dimethylamine sub-stitutions as seen in compound **12h** resulted in the loss of HDAC 8 inhibition and a low micromolar HDAC 6 activity, a near mirror image of the HDAC inhibition preference of **12g**. Finally, we found that the incorporation of *N,N*-dimethylamino group at the *para*-position of triazole containing 3-HPT **17a**, to afford compound **17b**, did not improve HDAC 8 selectivity.

Table 2. In Vitro HDAC Inhibition of Phenyl and Biphenyl HDACi[a]
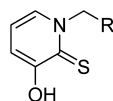
Compound	R	HDAC1 IC_{50} (nM)	HDAC6 IC_{50} (nM)	HDAC8 IC_{50} (nM)
7b		NI*	457 ± 27	1272±200
7c		NI	847 ± 188	4283±1548
12a		NI	957±159	2075±459
12b		NI	44%†	1701±717
12c		NI	372 ± 35	1907±771
12d		NI	454 ± 42	800±304
12e		NI	812 ± 286	2496±1180
12f		NI	306 ± 69	3105±1649
12g		NI	NI	2858±944
12h		NI	2390 ± 458	34%
12i		NI	2204 ± 355	2780±323
17a		NI	41%	1570±1067
17b		NI	1023 ± 99	1868±723
SAHA	-	38 ± 2	144 ± 23	232 ± 19

[a]*No significant Inhibition (below 20% Inhibition). †% inhibition of the compounds at 10 μM are given if the IC_{50} was above 10 μM.

Instead, it conferred HDAC 6 inhibition activity to **17b**. A similar substitution on the biphenyl congeners improved HDAC 8 inhibition but resulted in the loss of HDAC 6 inhibition (Table 2, comparing **12g** and **17b**). This observation suggests a possible divergence in the SARs of the triazole and biphenyl 3-HPT compounds. We describe the furtherance of our SAR studies on the triazole 3-HPT compounds in the next manuscript.

We then performed further docking analyses on representative compounds against HDAC 6 to gain a better understanding of the molecular basis of their stronger binding interaction with this HDAC isoform. We docked compounds **12a–f**, which showed a clear dependence of substitution pattern on HDAC inhibition activities (Table 2). The docked poses adopted by these compounds gave insights into the preference for *ortho*-substituents in the analogues (Figure 5). The biphenyl moieties of the *ortho*-substituted compounds **12c** and **12f** adopted a nearly indistinguishable orientation in which the cyano and methyl groups, respectively, are neatly nestled within a hydrophobic pocket at the enzyme outer rim where they could engage in potentially stabilizing hydrophobic interactions with amino acid residues including Tyr782 and Phe620. In contrast, the cyano and methyl groups of compounds **12a**, **12b**, **12d**, and **12e** are not oriented toward the same hydrophobic pocket. Instead, they are solvent exposed, thus missing the potentially stabilizing hydrophobic
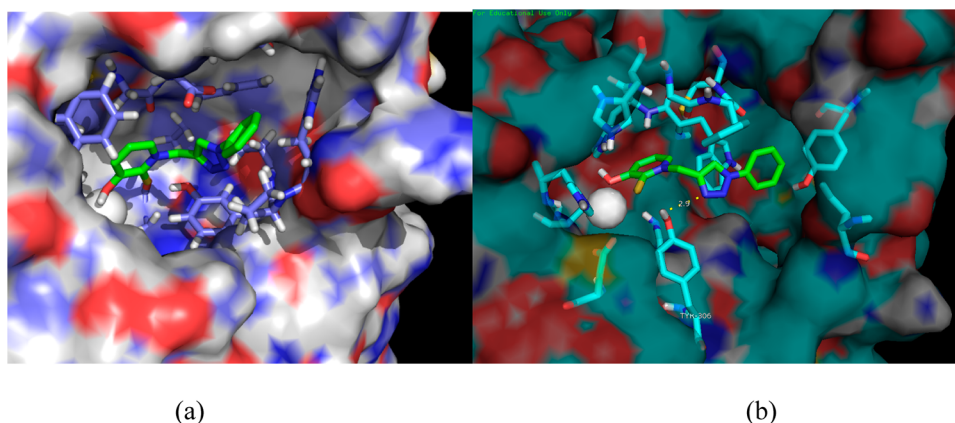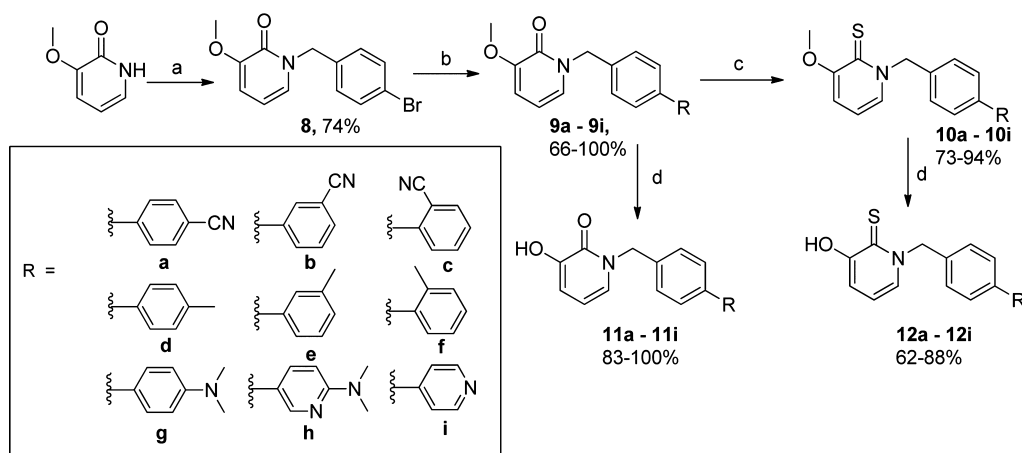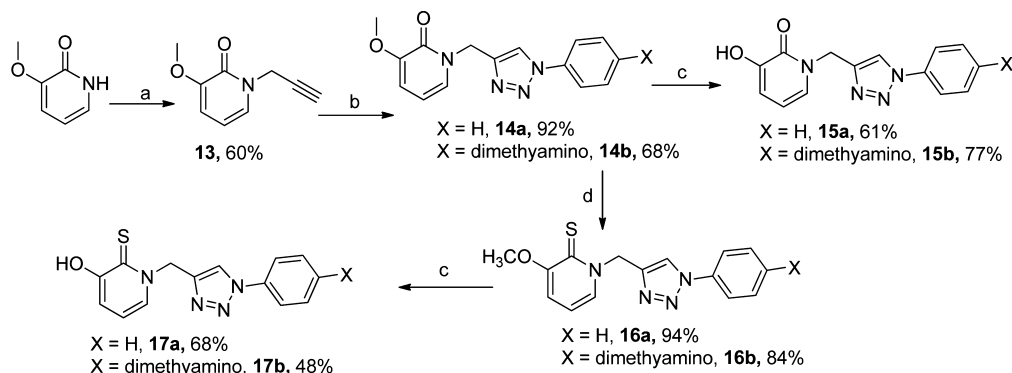
Figure 4. Docked structures of 3-HPT diaryl **17a** at the active site of (a) HDAC 6 and (b) HDAC 8. Note that the placement of the triazole ring of **17a** could facilitate H-bonding interaction with the OH-group of HDAC 8 Tyr306.

Scheme 2. Synthesis of the Biphenyl 3-HP and 3-HPT-Based HDACi[a]

[a](a) 4-Bromobenzylbromide, K$_2$CO$_3$, THF, reflux; (b) R-B(OH)$_2$, Pd(PPh$_3$)$_4$, K$_2$CO$_3$, toluene:ethanol:H$_2$O, 80 °C; (c) Lawesson's reagent, toluene, reflux; (d) BBr$_3$, CH$_2$Cl$_2$.

Scheme 3. Synthesis of the Triazole 3-HP and 3-HPT-Based HDACi[a]

[a](a) Propargyl bromide, K$_2$CO$_3$, THF, reflux; (b) azido intermediates (phenyl azide, 4-azido-N,N-dimethylaniline), CuI, DIPEA, THF; (c) BBr$_3$, CH$_2$Cl$_2$; (d) Lawessons' reagent, toluene, reflux.

interactions enjoyed by their *ortho*-substituted congeners. This observation might explain the enhanced potency of **12c** and **12f** against HDAC 6 compared to **12a**, **12b**, **12d**, and **12e** (Table 2).

To further probe the structural basis for the hindrance of the proper accommodation of these 3HPT-based compounds at HDAC 1 active site, we docked compound **12d**, analogue with

potent HDAC 6 and 8 inhibition activities but lacking the potentially obstructive ortho/meta substitution, against HDAC 1 homology model and HDLP. We observed that **12d** was incapable of entering HDAC 1 pocket to chelate the zinc at the active site, instead it was bound to the residues at the surface of the binding pocket. While **12d** bound to mutiple spots on HDLP, none of its conformation was able to present the 3HPT
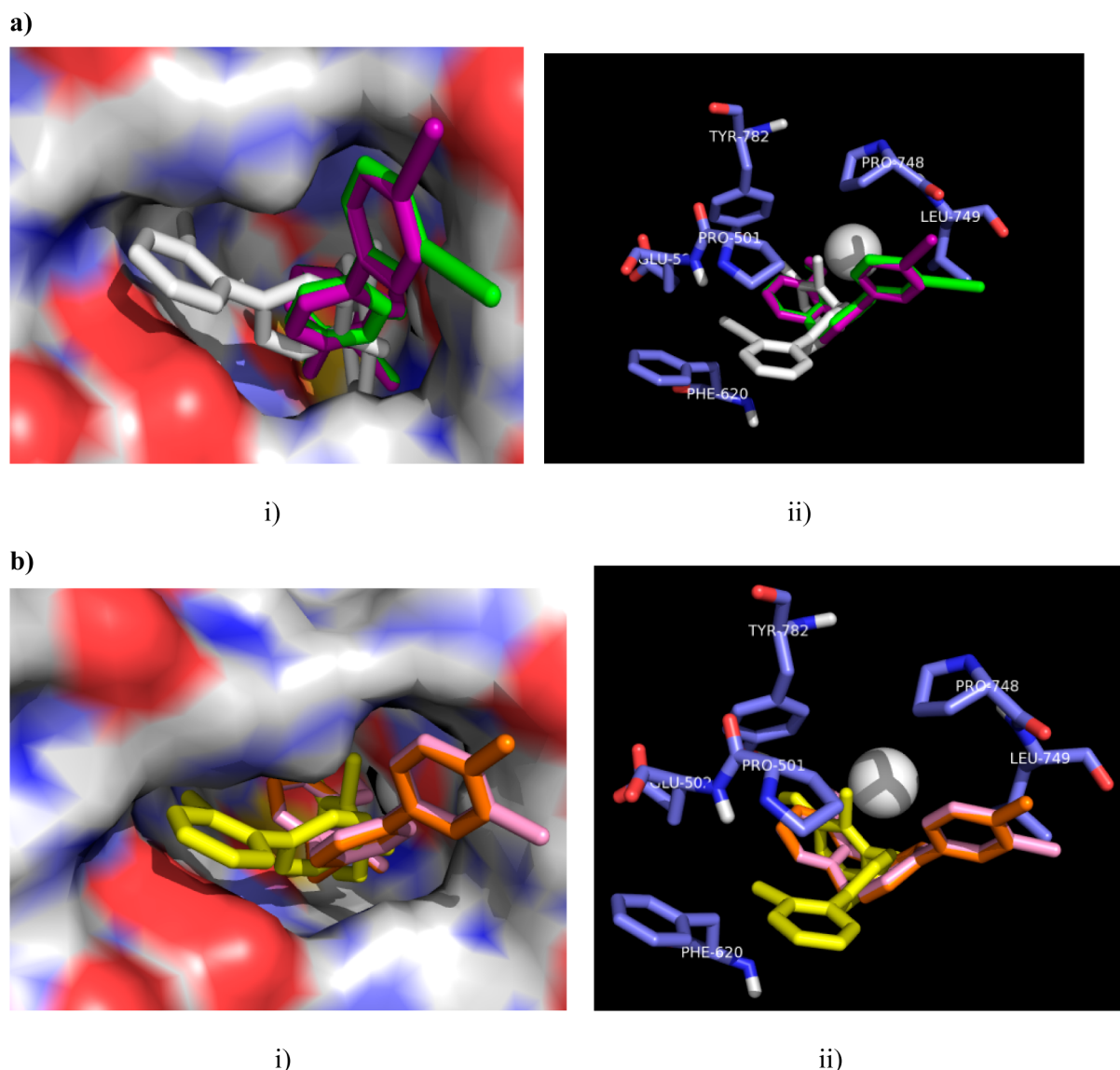
Figure 5. Docked poses adopted by 3-HPT compounds **12a−f** at HDAC 6 active site. (a) Overlay of low energy conformations of **12a** (purple), **12b** (green), and **12c** (white): (i) surface view, (ii) ball and stick model showing crucial residues at enzyme outer rim hydrophobic pocket. (b) Overlay of low energy conformations of **12d** (orange), **12e** (pink), and **12f** (yellow): (i) surface view, (ii) ball and stick model showing crucial residues at enzyme outer rim hydrophobic pocket.

ZBG for chelation to the active site zinc ion (Supporting Information Figure S6). This in silico observation may further explain the lack of activity of this class of compounds against HDAC 1.

In Vitro Cell Growth Inhibition. We tested several of the compounds in proliferation assays of cancer cell lines DU-145 (androgen independent prostate cancer), LNCaP (androgen dependent prostate cancer), and the T-cell leukemia cell line Jurkat. The compounds included a selective HDAC8 inhibitor (**12g**), compounds that inhibited both HDAC6 and 8 (**12c** and **12f**) and a triazole-based inhibitor selective for HDAC8 (**17a**).

Although 3-HPT **2** is active against HDAC6 and to some extend HDAC8, it is inactive against the three cancer cell lines tested (Table 3). The discrepancy between the HDAC inhibition profile and the antiproliferative activity of 3-HPT may be due to solubility problems that limit its diffusion across the cell membrane.[37] Against DU-145, a prostate cancer line known to be responsive to HDACi such as SAHA or TSA, only

Table 3. Cell Viability Assay: IC$_{50}$ of Selected Compounds against Various Cancer Cell Lines

	cellular IC$_{50}$ (μM)			
compd	DU-145	LNCaP	Jurkat	Jurkat J.gamma1
3-HPT (**2**)	NI[a]	NI	NI	NT[b]
12g	>20	16.23 ± 1.11	10.62 ± 0.67	NI
12c	>20	14.65 ± 0.84	8.95 ± 0.69	NT
12f	13.59 ± 2.91	7.75 ± 0.73	3.19 ± 0.30	NI
17a	>20	13.11 ± 1.51	4.68 ± 0.34	NI
SAHA	2.49 ± 0.2	2.31 ± 0.74	1.49 ± 0.10	NI

[a]NI = no inhibition. [b]NT = not tested.

12f exhibited a weak activity; all other compounds were inactive at the highest tested concentration of 20 μM (Table 3). SAHA, which was used as a positive control, had IC$_{50}$ value comparable to that reported in the literature.[38]

The compounds were more active on the LNCaP cell line (Table 3). Compound **12f** is the most potent of the biphenyls, followed by **12c** and **12g**. Interestingly, the cell growth inhibition activity of the triazolyl compound **17a** is comparable to that of **12c** although **17a** is a weak HDAC 6 inhibitor (only 41% inhibition at 10 μM, Table 2). With the exception of **17a**, the observed trend of the cell growth inhibition activity mirrored that of the HDAC 6 inhibition seen in Table 2. This may be due to the fact that LNCaP cells are sensitive to the acetylation state of HSP90. Hyperacetylation of HSP90, induced by the tested 3-HPT derived HDACi, attenuates its interactions with proteins such as androgen receptors, which are key to the survival of LNCaP cells.[39,40]

Because T-cell-derived leukemia cell line Jurkat has been previously shown to be sensitive to selective HDAC 8 inhibitor,[41] we investigated the effects of our compounds on the viability of Jurkat cells. Overall, all the compounds, excluding 3-HPT, inhibit Jurkat cell growth with single-digit micromolar IC$_{50}$ values (Table 3). Compound **12f**, which inhibited both HDAC 6 and HDAC 8, is the most potent against the Jurkat cells (IC$_{50}$ = 3.19 μM) in a similar manner to its activity against LNCaP cells. The HDAC 8 selective compounds **12g** and **17a** are cytotoxic to the Jurkat cells with **17a**, the more potent HDAC 8 inhibitor of the two, being twice as potent. The enhanced cytotoxicity of **17a** relative to **12g** could suggest a causal relationship between HDAC 8 inhibition and the apoptotic effect against Jurkat cells.

The apoptotic pathway, which is mediated by the activity of phospholipase C γ1 (PLCγ1) in Jurkat cells, is believed to be initiated by an HDAC 8 specific enzyme.[41] Balasubramanian and co-workers reported that an HDAC 8 specific inhibitor, PCI-34051, lost its ability to induce apoptosis in Jurkat J.gamma1, a mutant Jurkat cell line which has no detectable PLCγ1 activity.[41] To further delineate the contribution of HDAC 8 to apoptosis induction, we probed the effect of compounds **12f**, **12g**, **17a**, and SAHA on the viability of Jurkat J.gamma1 cells. As anticipated for HDAC 8 selective inhibitors, compounds **12g** and **17a** are devoid of antiproliferative activity against Jurkat J.gamma1 (Table 3). Quite unexpectedly, **12f** (which inhibited HDACs 6 and 8) and SAHA (a much broader HDACi) are noncytotoxic to this mutant Jurkat cell line. The inactivity of **12g** and **17a** against Jurkat J.gamma1 confirmed HDAC 8 contribution to their bioactivity. In the Jurkat cell line, Ca^{2+} released through PLCγ1 triggers cascade of events resulting in mitochondrial cytochrome c release and caspase-dependent apoptosis. The defect in intracellular Ca^{2+} mobilization in the Jurkat J.gamma1 mutant may also explain the inactivity of **12f** and SAHA, as this prevents the increase in cytochrome c release observed in the wild-type Jurkat.[41] Alternatively, the observed dependence of the cytotoxicity activity of **12f** and SAHA on PLCγ1 activity may be due to the attenuation of caspase-dependent apoptosis which is crucial for the cytotoxicity of HDACi.

On the basis of the foregoing, there is a discrepancy between HDAC inhibition and the whole cell activities of some of the tested compounds. This is to be expected as it is not unusual to observe such a lack of correlation between the two experiments. It is, however, possible that compound solubility could play a significant role in cell penetration which may perturb the whole cell activities. Therefore, we estimated the solubility of all compounds tested in cell growth inhibition assay to probe for the effect of solubility on antiproliferative activity. Among these compounds, 3HPT and **12g** had solubility less than 65 μg/mL

(Supporting Information Figure S7 and Table S1). For these two compounds, poor solubility may explain the lack of cellular activity.[42,43] However, the solubilities of the other compounds tested are beyond the suggested threshold that limits cellular activity.[42,43] Hence, the reduced efficacy of many of these compounds may be attributable to factors other than solubility issues.

Intracellular Target Validation. Of the compounds tested for anticancer activity, **12f** is approximately 10-fold selective toward HDAC 6 compared to HDAC 8. To probe the contribution of HDAC 6 inhibition to the cytotoxic activity of **12f**, we determined the level of tubulin acetylation, a common marker for intracellular HDAC 6 inhibition, in LNCaP cells through Western blot. We observed that **12f** led to an increase in tubulin acetylation in LNCaP cells at IC$_{50}$ concentration and at 20 μM (Figure 6), while SAHA, used as a positive control,
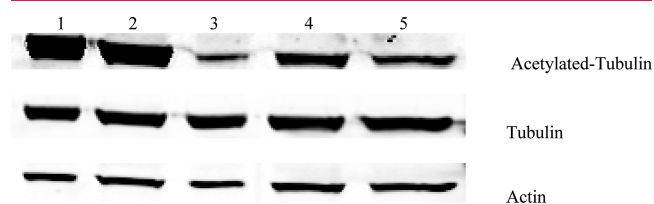

Figure 6. Western blot analysis of tubulin acetylation (HDAC6 inhibition) in LNCaP cell line. Lanes: 1, SAHA (20 μM); 2, SAHA IC$_{50}$ (2.31 μM); 3, control; 4, **12f** (20 μM); 5, **12f** IC$_{50}$ (7.75 μM).

showed concentration dependent tubulin hyperacetylation as observed before.[44] This data provides evidence for the involvement of intracellular HDAC 6 inhibition as part of the mechanisms of antiproliferative activity of **12f**.

CONCLUSION

We report that 3-hydroxypyridin-2-thione (3-HPT) is a novel ZBG that is compatible with HDAC inhibition. All of the 3-HPT-derived compounds reported herein are inactive against HDAC 1, but many possessed varying degrees of activity in inhibiting HDAC 6 and HDAC 8. Additionally, a subset of these compounds is cytotoxic to various cancer cell lines. The pattern of changes to key intracellular markers induced by representative members of these compounds confirmed the contribution of HDACs 6 and 8 to their bioactivity. To the best of our knowledge, this study described the first use of 3-HPT as ZBG for HDAC inhibition. Because of their anticipated immunity to many of the metabolic and pharmacokinetic liabilities that has beleaguered the hydroxamate ZBG, these 3-HPT-derived HDACi may display improved in vivo activity.

EXPERIMENTAL SECTION

Materials and Methods. Bromoalkanoic acid, benzyl bromide, 4-bromobenzylbromide, 4-(bromomethyl)-1,1′-biphenyl, 3-methoxy-2(1H)-pyridone, propargyl bromide, phenylacetylene, and representative boronic acids were purchased from either Sigma—Aldrich or Alfa—Aesar. Anhydrous solvents and other reagents were purchased and used without further purification. Analtech silica gel plates (60 F$_{254}$) were used for analytical TLC, and Analtech preparative TLC plates (UV 254, 2000 μm) were used for purification. UV light was used to examine the spots. Silica gel (200—400 mesh) was used in column chromatography. NMR spectra were recorded on a Varian-Gemini 400 magnetic resonance spectrometer. ^{1}H NMR spectra were recorded in parts per million (ppm) relative to the peak of CDCl$_3$, (7.24 ppm), CD$_3$OD (3.31 ppm), or DMSO-d_6 (2.49 ppm). ^{13}C spectra were recorded relative to the central peak of the CDCl$_3$ triplet (77.0 ppm),

CD$_3$OD (49.0 ppm), or the DMSO-d_6 septet (39.7 ppm) and were recorded with complete heterodecoupling. Multiplicities are described using the abbreviation: s, singlet; d, doublet; t, triplet; q, quartet; m, multiplet; app, apparent. High-resolution mass spectra were recorded at the Georgia Institute of Technology mass spectrometry facility in Atlanta. All final 3HPT-based compounds were established to be >95% pure using HPLC. These HPLC analyses were done on a Beckman Coulter instrument with a Phenomenex RP C-18 column (250 mm × 4.6 mm), using water (solvent A) and acetonitrile (solvent B) gradient, starting from 40% to 80% of B over 20 min. The flow rate was 1 mL/min, and detection was at 379 nm. Phenyl azide and 4-azido-*N,N*-dimethylaniline were synthesized as previously reported.[45,46] DU-145, LNCaP, and Jurkat J.gamma1 were obtained from ATCC (Manassas, VA, USA), and Jurkat E6-1 cell line was kindly donated by Dr. John McDonald and grown on recommended medium supplemented with 10% fetal bovine serum (Global Cell Solutions, Charlottesville, VA, USA) at 37 °C in an incubator with 5% CO$_2$. Mouse antiacetylated α-tubulin antibody was obtained from Invitrogen (Life Technologies, Grand Island, NY, USA), rabbit antiactin, and rabbit antitubulin α antibodies were purchased from Sigma-Aldrich (St. Louis, MO, USA). Secondary antibodies, goat antirabbit conjugated to IRDye680, and goat antimouse conjugated to IRDye800 were purchased from LI-COR Biosciences (Lincoln, NE, USA). The CellTiter 96 AQueous One Solution Cell Proliferation assay (MTS) kit was purchased from Promega (Madison, WI, USA).

Histone Deacetylase Inhibition. The HDAC activity in presence of various compounds was assessed using the SAMDI mass spectrometry. As a label-free technique, SAMDI is compatible with a broad range of native peptide substrates without requiring potentially disruptive fluorophores. To obtain IC$_{50}$ values, we incubated isoform-optimized substrates (50 μM) with enzyme (250 nM) and inhibitor (at concentrations ranging from 10 nM to 1.0 mM) in 96-well microtiter plates (60 min, 37 °C). Solution-phase deacetylation reactions were quenched with trichostatin A (TSA) and transferred to SAMDI plates to immobilize the substrate components. SAMDI plates were composed of an array of self-assembled monolayers (SAMs) presenting maleimide in standard 384-well format for high-throughput handling capability. Following immobilization, plates were washed to remove buffer constituents, enzyme, inhibitor, and any unbound substrate and analyzed by MALDI mass spectrometry using automated protocols.[34] Deacetylation yields in each triplicate sample were determined from the integrated peak intensities of the molecular ions for the substrate and the deacetylated product ion by taking the ratio of the former over the sum of both. Yields were plotted with respect to inhibitor concentration and fitted to obtain IC$_{50}$ values for each isoform–inhibitor pair.

Cell Viability Assay. DU-145 cells were maintained in EMEM supplemented with 10% FBS while all other cell lines were maintained in RPMI 1640 supplemented with 10% FBS. DU-145 and LNCaP cells were incubated on a 96-wells plate for 24 h prior to the drug treatment, while Jurkat and Jurkat J.gamma1 cells were incubated in media containing the various compounds for 72 h. Cell viability was measured using the MTS assay according to manufacturer protocol. The DMSO concentration in the cell media during the cell viability experiment was maintained at 0.1%.

Western Blot Analysis for Tubulin Acetylation. LNCaP cells were plated for 24 h and treated with various concentrations of compounds for 4 h. The cells were washed with PBS buffer and resuspended in CelLyticM buffer containing a cocktail of protease inhibitor (Sigma-Aldrich, St. Louis, MO, USA). Following quantification through a Bradford protein assay, an equal amount of protein was loaded onto an SDS-page gel (Bio-Rad, Hercules, CA, USA) and resolved by electrophoresis at a constant voltage of 100 V for 2 h. The gel was transfer onto a nitrocellulose membrane and probed for acetylated tubulin, tubulin, and actin as loading control.

Statistical Analysis. The values reported as mean ± standard deviation from at least two independent triplicate experiments. A student's *t* test was performed in Excel, and results with *p* value less than 5% were considered statistically different.

*1-Methyl-3-methoxypyridin-2-one (**4a**).* To a stirring mixture of 3-methoxypyridin-2-one (0.20 g, 1.6 mmol) and KOH (0.18 g, 3.2 mmol) in methanol was added MeI (0.68 g, 4.8 mmol) dropwise in a round-bottom flask. Stirring continued overnight at room temperature, during which a quantitative consumption of starting materials was observed. The reaction mixture was diluted with water (35 mL) and CHCl$_3$ (40 mL), and the two layers were separated. The organic layer was washed with water (35 mL) and brine (30 mL) and dried over Na$_2$SO$_4$. Solvent was evaporated off in vacuo to yield **4a** (0.20 g, 89%) as a colorless oil. ^{1}H NMR (400 MHz, CDCl$_3$) δ 6.66 (m, 1H), 6.35 (d, *J* = 7.4 Hz, 1H), 5.83 (t, *J* = 7.1 Hz, 1H), 3.52 (s, 3H), 3.28 (s, 3H). ^{13}C NMR (100 MHz, CDCl$_3$) δ 158.0, 149. 6, 128.8, 111.9, 104.3, 55.44, 37.1.

*1-Benzyl-3-methoxypyridin-2-one (**4b**).* To a stirring mixture of 3-methoxypyridin-2-one (0.20 g, 1.6 mmol) and K$_2$CO$_3$ (0.66 g, 4.8 mmol) in DMF (8 mL) was added benzyl bromide (0.33 g, 1.92 mmol) dropwise in a condenser equipped round-bottom flask. Reaction mixture was heated at 100 °C overnight. The reaction mixture was cooled down, diluted with water (40 mL) and CHCl$_3$ (50 mL), and the two layers were separated. The organic layer was washed with water (3 × 40 mL) and brine (30 mL) and dried over Na$_2$SO$_4$. Solvent was evaporated off in vacuo to yield **4b** (0.26 g, 75%) as a colorless oil without any further purification needed. ^{1}H NMR (400 MHz, CDCl$_3$) δ 7.26 (m, 5H), 6.85 (dd, *J* = 6.9, 1.7 Hz, 1H), 6.54 (dd, *J* = 7.5, 1.6 Hz, 1H), 6.03 (m, 1H), 5.13 (s, 2H), 3.76 (s, 3H). ^{13}C NMR (100 MHz, CDCl$_3$) δ 157.9, 150.1, 136.3, 128. 6, 128.0, 127.7, 111.8, 104.8, 104.8, 55.6, 51.6.

*1-(1,1′-Biphenylmethyl)-3-methoxypyridin-2-one (**4c**).* The reaction of 3-methoxypyridin-2-one (0.20 g, 1.6 mmol), K$_2$CO$_3$ (0.66 g, 4.8 mmol), and (4-bromomethyl)-1,1′-biphenyl (0.47 g, 1.92 mmol) in DMF (8 mL) according to method described for the synthesis of **4b** followed by column chromatography in CH$_2$Cl$_2$ with acetone (0−15% gradient) followed by CH$_2$Cl$_2$ with MeOH (0−5% gradient) afforded **4c** (0.35 g, 76%) as a colorless oil. ^{1}H NMR (400 MHz, CDCl$_3$) δ 7.48 (dd, *J* = 25.9, 20.6 Hz, 4H), 7.32 (m, 5H), 6.88 (m, 1H), 6.54 (d, *J* = 7.2 Hz, 1H), 6.04 (t, *J* = 7.1 Hz, 1H), 5.16 (s, 2H), 3.76 (s, 3H). ^{13}C NMR (100 MHz, CDCl$_3$) δ 157.9, 150.0, 140.5, 140.2, 135.3, 128.5, 128.4, 127.7, 127.2, 127.1, 126.7, 111.8, 104.8, 55. 6, 51.4.

*1-Methyl-3-hydroxypyridin-2-one (**5a**).* To a solution of **4a** (0.10 g, 0.68 mmol) in dry CH$_2$Cl$_2$ (8 mL) was slowly added 1 M BBr$_3$ (0.82 mL) at −30 °C under inert atmosphere. The reaction mixture was stirred for 48 h at room temperature. The mixture was again cooled to −30 °C, and MeOH (5 mL) was slowly added to the mixture. After evaporation of solvent, the residue was adjusted to pH 7 with 1 M NaOH and then extracted with CHCl$_3$ (3 × 30 mL). The combined organic layer was dried over Na$_2$SO$_4$, and solvent was evaporated in vacuo. The residue was purified by prep-TLC, eluting with CH$_2$Cl$_2$:acetone:MeOH (10:1:0.2), to give **5a** (61 mg, 72%) as an off-white solid. ^{1}H NMR (400 MHz, CDCl$_3$) δ 7.92 (s, 1H), 6.78 (dd, *J* = 11.1, 7.1 Hz, 2H), 6.10 (t, *J* = 7.0 Hz, 1H), 3.57 (s, 3H). ^{13}C NMR (100 MHz, CDCl$_3$) δ 158.8, 146. 7, 127.6, 114.4, 106.7, 37.3. HRMS (EI) calcd for C$_6$H$_7$NO$_2$ [M]$^+$ 125.0477, found 125.0477.

*1-Benzyl-3-hydroxypyridin-2-one (**5b**).* The reaction of **4b** (0.15 g, 0.55 mmol) with 1 M BBr$_3$ (0.66 mL) in dry CH$_2$Cl$_2$ (5 mL) within 48 h as described for **5a** afforded **5b** (0.13 g, 90%) as a slightly brownish solid. ^{1}H NMR (400 MHz, CDCl$_3$) δ 7.31 (m, 5H), 6.83 (m, 3H), 6.14 (t, *J* = 7.1 Hz, 1H), 5.19 (s, 2H). ^{13}C NMR (100 MHz, CDCl$_3$) δ 158.6, 146. 8, 135.8, 128.7, 128.0, 126.5, 113.9, 107.0, 52.2. HRMS (EI) calcd for C$_{12}$H$_{11}$NO$_2$ [M]$^+$ 201.0792, found 201.0790.

*1-(1,1′-Biphenylmethyl)-3-hydroxypyridin-2-one (**5c**).* The reaction of **4c** (0.13 g, 0.43 mmol) with 1 M BBr$_3$ (0.51 mL) in dry CH$_2$Cl$_2$ (7 mL) within 48 h as described for **5a** afforded **5c** (0.10 g, 82%) as a slightly brownish solid. ^{1}H NMR (400 MHz, DMSO-d_6) δ 9.06 (s, 1H), 7.61 (d, *J* = 7.5 Hz, 4H), 7.36 (m, 6H), 6.70 (d, *J* = 6.5 Hz, 1H), 6.12 (t, *J* = 6.9 Hz, 1H), 5.16 (s, 2H). ^{13}C NMR (100 MHz, DMSO-d_6) δ 147.0, 139.8, 139.5, 136.6, 128.9, 128.4, 128.2, 127.5, 126.9, 126.7, 114.8, 105.6, 51.1. HRMS (EI) calcd for C$_{18}$H$_{15}$NO$_2$ [M]$^+$ 277.1101, found 277.1103.

*1-Benzyl-3-methoxypyridin-2-thione (**6b**).* A suspension of **4b** (0.06 g, 0.28 mmol) and Lawesson's reagent (0.07 g, 0.17 mmol) in

toluene (10 mL) was heated at reflux overnight. The reaction mixture was cooled to room temperature, and solvent was evaporated in vacuo. The crude solid was purified on prep-TLC, eluting with CH₂Cl₂:acetone:MeOH (5:1:0.2), to give **6b** (53 mg, 82%) as a yellow solid. ^{1}H NMR (400 MHz, CDCl₃) δ 7.30 (m, 6H), 6.65 (d, J = 7.7 Hz, 1H), 6.54 (t, J = 7.0 Hz, 1H), 5.89 (s, 2H), 3.88 (s, 3H). ^{13}C NMR (100 MHz, CDCl₃) δ 173.2, 159.0, 135.2, 131.7, 128.7, 128.0, 128.0, 111.6, 109.6, 58.8, 56.6. HRMS (EI) calcd for C₁₃H₁₃NOS [M]⁺ 231.0718, found 231.0716.

1-(1,1′-Biphenylmethyl)-3-methoxypyridin-2-thione (6c). The reaction of **4c** (0.13 g, 0.44 mmol) and Lawesson's reagent (0.11 g, 0.27 mmol) in toluene according to method described for the synthesis of **6b** afforded **6c** (122 mg, 88%) as a yellow solid. ^{1}H NMR (400 MHz, CDCl₃) δ 7.52 (m, 1H), 7.35 (m, 2H), 6.66 (dd, J = 7.8, 1.3 Hz, 1H), 6.55 (dd, J = 7.8, 6.6 Hz, 1H), 5.93 (s, 1H), 3.89 (s, 1H). ^{13}C NMR (100 MHz, CDCl₃) δ 173.1, 159.0, 140.8, 140.2, 134.1, 131.7, 128.6, 128.4, 127.4, 127.3, 126.8, 111.6, 109.7, 104.8, 58.5, 56.6. HRMS (EI) calcd for C₁₉H₁₇NOS [M]⁺ 307.1031, found 307.1029.

1-Benzyl-3-hydroxypyridin-2-thione (7b). The reaction of **6b** (0.05 g, 0.21 mmol) with 1 M BBr₃ (0.66 mL) in dry CH₂Cl₂ (5 mL) within 48 h as described for **5a** afforded **7b** (34 mg, 72%) as an olive-green solid. Retention time 21.27 min (solvent gradient: 40−80% solvent B in 20 min then constant 80% B for 5 min). ^{1}H NMR (400 MHz, CD₃OD) δ 7.34 (m, 3H), 6.84 (m, 1H), 5.83 (d, J = 49.5 Hz, 1H). ^{13}C NMR (100 MHz, CDCl₃) δ 164.7, 134.2, 129.0, 128.5, 128.1, 127.8, 126.7, 118.8, 118.3, 62.2. HRMS (EI) calcd for C₁₂H₁₁NOS [M]⁺ 217.0561, found 217.0762.

1-(1,1′-Biphenylmethyl)-3-hydroxypyridin-2-thione (7c). The reaction of **6c** (0.10 g, 0.32 mmol) with 1 M BBr₃ (0.48 mL) in dry CH₂Cl₂ (5 mL) within 48 h as described for **5a** afforded **7c** (74 mg, 90%) as an olive-green solid. Retention time 15.37 min (solvent gradient: 40−80% solvent B in 20 min then constant 80% B for 5 min) ^{1}H NMR (400 MHz, CD₃OD) δ 7.39 (m, 9H), 6.88 (m, 3H), 5.86 (s, 2H). ^{13}C NMR (100 MHz, CDCl₃) δ 169.9, 155.2 141.3, 140.2, 133.5, 130.9, 128.7, 128.5, 127.7, 127. 5, 126.9, 113.7, 111.9, 95.8. HRMS (EI) calcd for C₁₈H₁₅NOS [M]⁺ 293.0874, found 293.0873.

1-(4-Bromobenzyl)-3-methoxypyridin-2(1H)-one (8). To a stirring reaction mixture of 3-methoxypyridin-2-one (2.00 g, 16 mmol) and K₂CO₃ (4.42 g, 32 mmol) in THF was added 4-bromobenzyl bromide (5.20 g, 20.8 mmol) slowly. The reaction mixture was the heated at reflux overnight, cooled down, and then partitioned between CH₂Cl₂ (120 mL) and water (60 mL). The organic layer was separated, washed with water (2 × 60 mL) and brine (1 × 40 mL), and dried on Na₂SO₄. Solvent was evaporated in vacuo, and the crude yellowish solid was triturated with hexanes to give **8** (3.49 g, 74%) as a white solid without further purification. ^{1}H NMR (400 MHz, CDCl₃) δ 7.45−7.29 (m, 2H), 7.15 (dd, J = 7.4, 1.2 Hz, 2H), 6.84 (dd, J = 6.9, 1.7 Hz, 1H), 6.55 (dd, J = 7.4, 1.5 Hz, 1H), 6.21−5.79 (m, 1H), 5.06 (s, 2H), 3.76 (s, 3H). ^{13}C NMR (100 MHz, CDCl₃) δ 158.0, 150.3, 135.5, 131.8, 129.9, 127.7, 121.9, 112.0, 105.2, 55.8, 51.41. HRMS (EI) calcd for C₁₃H₁₂BrNO₂ [M]⁺ 293.0051, found 293.0051.

Representative Procedure for Suzuki Coupling Reactions for Synthesis of 9-1-(4-Cyano-(1,1′-biphenylmethyl))-3-methoxyoxypyridin-2-one (9a). Compound **8** (0.26 g, 0.86 mmol), (4-cyanophenyl)boronic acid (0.14 g, 0.95 mmol), 2 M aq K₂CO₃ (0.24 g, 1.73 mmol), toluene (8 mL), EtOH (4 mL), and water (4 mL) were added into reaction flask equipped with magnetic stirrer and water condenser. The resulting suspension was degassed for 10 min by sparging with argon gas. Pd(PPh₃)₄ (2.5 mol %) was added, and the reaction mixture was heated at reflux overnight under argon atmosphere. After cooling to room temperature, CH₂Cl₂ was added (50 mL) and the mixture was extracted with water (40 mL) and brine (20 mL) and dried on Na₂SO₄. Solvent was evaporated in vacuo, and the residue was purified by column chromatography eluting with CHCl₃:acetone:MeOH (first with 5−20% acetone gradient, no MeOH followed by 1−8% MeOH step gradient) to give **9a** (0.42 g, 78%) as an off-white solid. ^{1}H NMR (CDCl₃, 400 MHz) δ 7.60 (m, 4H), 7.40 (m, 4H), 6.90 (dd, J = 6.8, 1.6 Hz, 1H), 6.55 (dd, J = 7.6, 1.6 Hz, 1H), 6.07 (t, J = 7.2 Hz, 1H), 5.16 (s, 2H), 3.75 (s, 3H). ^{13}C NMR (100 MHz, CDCl₃) δ 158.1, 150.3, 145.0, 138.6, 137.1, 132. 6, 132.0, 128.9,

128.6, 128.4, 128.0, 127.6, 127.5, 118.9, 112.1, 110.9, 105.2, 56.2, 51.8. HRMS (EI) calcd for C₂₀H₆N₂O₂ [M]⁺ 316.1212, found 316.1210.

1-(3-Cyano-(1,1′-biphenylmethyl))-3-methoxyoxypyridin-2-one (9b). The reaction of **8** (0.25 g, 0.85 mmol), (3-cyanophenyl)boronic acid (0.14g, 0.93 mmol), 2 M aq K₂CO₃ (0.23 g, 1.69 mmol), and Pd(PPh₃)₄ (2.5 mol %) according to method described for the synthesis of **9a** within 18 h afforded **9b** (175 mg, 66%) as a white solid. ^{1}H NMR (400 MHz, CDCl₃) δ 7.70 (m, 2H), 7.48 (m, 6H), 6.92 (dd, J = 6.9, 1.6 Hz, 1H), 6.57 (dd, J = 7.4, 1.4 Hz, 1H), 6.08 (t, J = 7.2 Hz, 1H), 5.16 (s, 2H), 3.76 (s, 3H). ^{13}C NMR (100 MHz, CDCl₃) δ 158.1, 150.2, 141.7, 138.3, 136.8, 131.4, 130.8, 130. 5, 129.7, 128.9, 128.0, 127.4, 118.8, 112.8, 112.1, 105.3, 55.8, 51.7. HRMS (EI) calcd for C₂₀H₁₆N₂O₂ [M]⁺ 316.1212, found 332.1216.

1-(2-Cyano-(1,1′-biphenylmethyl))-3-methoxyoxypyridin-2-one (9c). The reaction of **8** (0.15 g, 0.50 mmol), (2-cyanophenyl)boronic acid (0.09 g, 0.60 mmol), 2 M aq K₂CO₃ (0.14 g, 1.69 mmol), and Pd(PPh₃)₄ (2.5 mol %) according to method described for the synthesis of **9a** within 18 h afforded **9c** (118 mg, 75%) of white solid. ^{1}H NMR (400 MHz, CDCl₃) δ 7.72 (m, 1H), 7.60 (m, 1H), 7.45 (m, 2H), 6.94 (dd, J = 6.9, 1.7 Hz, 1H), 6.60 (dd, J = 7.4, 1.6 Hz, 1H), 6.10 (t, J = 7.2 Hz, 1H), 5.21 (s, 1H), 3.80 (s, 1H). ^{13}C NMR (100 MHz, CDCl₃) δ 158.0, 150.2, 144.7, 137. 6, 136.9, 133.6, 132. 8, 129.9, 129.0, 128.3, 127.9, 127.6, 118.5, 112.0, 110.9, 105.1, 55.7, 51.6. HRMS (EI) calcd for C₂₀H₁₆N₂O₂ [M]⁺ 316.1212, found 316.1201.

1-(4-Methyl-(1,1′-biphenylmethyl))-3-methoxyoxypyridin-2-one (9d). The reaction of **8** (0.25g, 0.85 mmol), p-tolylboronic acid (0.14g, 1.02 mmol), 2 M aq K₂CO₃ (0.23g, 1.69 mmol), and Pd(PPh₃)₄ (2.5 mol %) according to method described for the synthesis of **9a** within 18 h afforded **9d** (259 mg, quantitative) as a white solid. ^{1}H NMR (400 MHz, CDCl₃) δ 7.49 (d, J = 8.1 Hz, 2H), 7.42 (d, J = 8.1 Hz, 2H), 7.33 (d, J = 8.1 Hz, 2H), 7.19 (d, J = 8.0 Hz, 2H), 6.88 (dd, J = 6.9, 1.6 Hz, 1H), 6.54 (dd, J = 7.4, 1.4 Hz, 1H), 6.03 (t, J = 7.2 Hz, 1H), 5.15 (s, 2H), 3.76 (s, 3H), 2.34 (s, 3H). ^{13}C NMR (100 MHz, CDCl₃) δ 157.8, 149.9, 140.4, 137.3, 136.9, 134.9, 129.2, 128.4, 127.7, 126.9, 126.5, 111.8, 104. 8, 55.5, 51.3, 20.8. HRMS (EI) calcd for C₂₀H₁₉NO₂ [M]⁺ 305.1416, found 305.1422.

1-(3-Methyl-(1,1′-biphenylmethyl))-3-methoxyoxypyridin-2-one (9e). The reaction of **8** (0.20 g, 0.68 mmol), m-tolylboronic acid (0.11 g, 0.82 mmol), 2 M aq K₂CO₃ (0.19 g, 1.36 mmol), and Pd(PPh₃)₄ (2.5 mol %) according to method described for the synthesis of **9a** within 18 h afforded **9e** (259 mg, quantitative) as a white solid. ^{1}H NMR (400 MHz, CDCl₃) δ 7.49 (m, 1H), 7.29 (m, 2H), 7.11 (d, J = 7.2 Hz, 1H), 6.88 (dd, J = 6.9, 1.7 Hz, 1H), 6.53 (dd, J = 7.4, 1.6 Hz, 1H), 6.03 (t, J = 7.2 Hz, 1H), 5.15 (s, 1H), 3.75 (s, 1H), 2.35 (s, 1H). ^{13}C NMR (100 MHz, CDCl₃) δ 157.8, 149.9, 140.6, 140.2, 138.0, 135.1, 128.4, 128.3, 127.8, 127.7, 127.5, 127.1, 123.8, 111.8, 104.8, 55.5, 51.3, 21.2. HRMS (EI) calcd for C₂₀H₁₉NO₂ [M]⁺ 305.1416, found 305.1415.

1-(2-Methyl-(1,1′-biphenylmethyl))-3-methoxyoxypyridin-2-one (9f). The reaction of **8** (0.20 g, 0.68 mmol), O-tolylboronic acid (0.11 g, 0.82 mmol), 2 M aq K₂CO₃ (0.19 g, 1.36 mmol), and Pd(PPh₃)₄ (2.5 mol %) according to method described for the synthesis of **9a** within 18 h afforded **9f** (243 mg, 98%) as a white solid. ^{1}H NMR (400 MHz, CDCl₃) δ 7.31 (d, J = 7.9 Hz, 1H), 7.17 (m, 2H), 6.93 (m, 1H), 6.56 (dd, J = 7.4, 1.6 Hz, 1H), 6.06 (t, J = 7.2 Hz, 1H), 5.18 (s, 1H), 3.76 (s, 1H), 2.20 (s, 1H). ^{13}C NMR (101 MHz, CDCl₃) δ 158.1, 150.2, 141.5, 141.3, 135.2, 135.0, 130.3, 129.7, 129.5, 128.1, 127.9, 127.3, 125.8, 112.1, 105.1, 55.8, 51.8, 20. 5. HRMS (EI) calcd for C₂₀H₁₉NO₂ [M]⁺ 305.1416, found 305.1419.

1-(4-Dimethylamino-(1,1′-biphenylmethyl))-3-methoxyoxypyridin-2-one (9g). The reaction of **8** (0.25g, 0.85 mmol), (4-(dimethylamino)phenyl)boronic acid (0.17g, 1.02 mmol), 2 M aq K₂CO₃ (0.23g, 1.69 mmol), Pd(PPh₃)₄ (2.5 mol %) according to method described for the synthesis of **9a** within 18 h afforded **9g** (230 mg, 81%) as a white solid. ^{1}H NMR (400 MHz, CDCl₃) δ 7.46 (m, 4H), 7.29 (m, 2H), 6.86 (dd, J = 7.2, 2.0 Hz, 1H), 7.73 (m, 2H), 6.52 (dd, J = 7.2, 1.6 Hz, 1H), 6.01 (t, J = 7.2 Hz, 1H), 5.13 (s, 2H), 3.76 (s, 3H), 2.93 (s, 6H). ^{13}C NMR (100 MHz, CDCl₃) δ 157.9, 149.9, 149.7, 140.6, 133.8, 128.4, 128.0, 127.7, 127.3, 126.2, 112.4, 111.8,

104.7, 55.5, 51.3, 40.2. HRMS (EI) calcd for $C_{21}H_{22}N_2O_2$ [M]$^+$ 334.1681, found 334.1684.

1-(4-(6-(Dimethylamino)pyridin-3-yl)benzyl))-3-methoxyoxypyridin-2-one (9h). The reaction of **8** (0.43g, 1.44 mmol), (6-(dimethylamino)pyridine-3-yl)boronic acid (0.2 g, 1.20 mmol), 2 M aq K_2CO_3 (0.33g, 2.41 mmol), and Pd(PPh$_3$)$_4$ (2.5 mol %) according to method described for the synthesis of **9a** within 18 h afforded **9h** (335 mg, 83%) as a white solid. ^{1}H NMR (400 MHz, CDCl$_3$) δ 8.28 (d, J = 2.3 Hz, 1H), 7.51 (dd, J = 8.8, 2.5 Hz, 1H), 7.33 (d, J = 8.2 Hz, 2H), 7.22 (d, J = 8.2 Hz, 2H), 6.80 (dd, J = 6.9, 1.6 Hz, 1H), 6.44 (m, 2H), 5.94 (t, J = 7.2 Hz, 1H), 5.04 (s, 2H), 3.66 (s, 3H), 2.97 (s, 6H). ^{13}C NMR (100 MHz, CDCl$_3$) δ 158.1, 157.6, 149.7, 145.5, 137.8, 135.1, 134.2, 128.4, 127.5, 125.7, 123.2, 111.6, 105.2, 104.6, 55.4, 51.2, 37.7. HRMS (EI) calcd for $C_{20}H_{21}N_3O_2$ [M]$^+$ 335.1634, found 335.1635.

1-(4-(Pyridin-4-yl)benzyl)-3-methoxy-pyridin-2-one (9i). The reaction of **8** (0.25g, 0.85 mmol), pyrdin-4-ylboronic acid (0.12g, 1.02 mmol), 2 M aq K_2CO_3 (0.23g, 1.69 mmol), and Pd(PPh$_3$)$_4$ (2.5 mol %) according to method described for the synthesis of **9a** within 18 h afforded **9i** (203 mg, 82%) as a white solid. ^{1}H NMR (400 MHz, CDCl$_3$) δ 8.54 (dd, J = 4.5, 1.6 Hz, 2H), 7.48 (m, 2H), 7.36 (m, 4H), 6.87 (dd, J = 6.9, 1.7 Hz, 1H), 6.53 (dd, J = 7.4, 1.6 Hz, 1H), 6.03 (t, J = 7.2 Hz, 1H), 5.13 (s, 2H), 3.72 (s, 3H). ^{13}C NMR (100 MHz, CDCl$_3$) δ 157.8, 150.3, 150.0, 149.9, 147.4, 137.3, 137.3, 128.6, 127.7, 127.0, 121.2, 111.9, 105.0, 55.6, 51.4. HRMS (EI) calcd for $C_{18}H_{16}N_2O_2$ [M]$^+$ 292.1212, found 292.1205.

Representative Procedure for Thionation Reaction: Synthesis of 10-1-(4-Cyano-(1,1'-biphenylmethyl))-3-methoxyoxypyridin-2-thione (10a). A suspension of **9a** (0.13 g, 0.42 mmol) and Lawesson's reagent (0.10 g, 0.25 mmol) in toluene (10 mL) was heated at reflux overnight. The reaction mixture was cooled to room temperature, and solvent was evaporated in vacuo. The residue was purified on prep-TLC, eluting with CHCl$_3$:acetone:EtOH (12:1:0.2) to give **10a** (123 mg, 88%) as a yellow solid. ^{1}H NMR (CDCl$_3$, 400 MHz) δ 7.60 (m, 4H), 7.40 (m, 4H), 6.90 (dd, J = 6.8, 1.6 Hz, 1H), 6.55 (dd, J = 7.6, 1.6 Hz, 1H), 6.07 (t, J = 7.2 Hz, 1H), 5.16 (s, 2H), 3.75 (s, 3H). ^{13}C NMR (100 MHz, CDCl$_3$) δ 158.1, 150.3, 145.0, 138.6, 137.1, 132. 6, 132.0, 128.9, 128.6, 128.4, 128.0, 127.6, 127.5, 118.9, 112.1, 110.9, 105.2, 56.2, 51.8 HRMS (EI) calcd for $C_{20}H_{16}N_2OS$ [M]$^+$ 332.0983, found 332.0987.

1-(3-Cyano-(1,1'-biphenylmethyl))-3-methoxypyridin-2-thione (10b). The reaction of **9b** (0.11 g, 0.36 mmol) and Lawesson's reagent (0.09 g, 0.22 mmol) in toluene according to method described for the synthesis of **10a** afforded **10b** (113 mg, 95%) as a yellow solid. ^{1}H NMR (400 MHz, DMSO-d_6) δ 7.92 (m, 3H), 7.84 (m, 2H), 7.71 (d, J = 8.4 Hz, 2H), 7.36 (d, J = 8.8 Hz, 2H), 7.00 (m, 1H), 6.80 (m, 1H), 5.95 (s, 2H), 3.78 (s, 3H). ^{13}C NMR (100 MHz, CDCl$_3$) δ 173.4, 159.3, 144.8, 138.8, 135.8, 132.6, 131.8, 128.7, 127.6, 127.5, 118.8, 111.8, 111.0, 109.7, 58.6, 56.7. HRMS (EI) calcd for $C_{20}H_{16}N_2OS$ [M]$^+$ 332.0983, found 332.0984.

1-(2-Cyano-(1,1'-biphenylmethyl))-3-methoxyoxypyridin-2-thione (10c). The reaction of **9c** (0.09 g, 0.28 mmol) and Lawesson's reagent (0.07 g, 0.17 mmol) in toluene according to method described for the synthesis of **10a** afforded **10c** (72 mg, 77%) of yellow solid. ^{1}H NMR (400 MHz, CDCl$_3$) δ 7.74 (m, 1H), 7.63 (td, J = 7.7, 1.4 Hz, 1H), 7.45 (m, 2H), 6.71 (dd, J = 7.8, 1.3 Hz, 1H), 6.62 (dd, J = 7.8, 6.6 Hz, 1H), 6.00 (s, 1H), 5.28 (s, 1H), 3.93 (s, 1H). ^{13}C NMR (101 MHz, CDCl$_3$) δ 173.4, 159.2, 144.7, 137.8, 135.8, 133. 7, 132.9, 132.0, 130.0, 129.2, 128.3, 127.7, 118.6, 111.8, 111.0, 109.8, 58.6, 56.7. HRMS (EI) calcd for $C_{20}H_{16}N_2OS$ [M]$^+$ 332.0983, found 332.0981.

1-(4-Methyl-(1,1'-biphenylmethyl))-3-methoxyoxypyridin-2-thione (10d). The reaction of **9d** (0.12 g, 0.39 mmol) and Lawesson's reagent (0.09 g, 0.23 mmol) in toluene according to method described for the synthesis of **10a** afforded **10d** (117 mg, 94%) as a yellow solid. ^{1}H NMR (400 MHz, CDCl$_3$) δ 7.51 (m, 2H), 7.42 (m, 2H), 7.34 (m, 3H), 7.21 (dd, J = 8.4, 0.6 Hz, 2H), 6.66 (dd, J = 7.8, 1.2 Hz, 1H), 6.55 (dd, J = 7.8, 6.6 Hz, 1H), 5.92 (s, 2H), 3.89 (s, 3H), 2.36 (s, 3H). ^{13}C NMR (100 MHz, CDCl$_3$) δ 173.1, 159.0, 140.7, 137.3, 137.1, 133.8, 131.7, 129.3, 128.4, 127.1, 126.6, 111.6, 109.7, 58.5, 56.6, 20.9. HRMS (EI) calcd for $C_{20}H_{19}NOS$ [M]$^+$ 321.1187, found 321.1192.

1-(3-Methyl-(1,1'-biphenylmethyl))-3-methoxyoxypyridin-2-thione (10e). The reaction of **9e** (0.12 g, 0.37 mmol) and Lawesson's reagent (0.09 g, 0.23 mmol) in toluene according to method described for the synthesis of **10a** afforded **10e** (112 mg, 93%) as a yellow solid. ^{1}H NMR (400 MHz, CDCl$_3$) δ 7.53 (m, 1H), 7.33 (m, 2H), 7.14 (dd, J = 7.1, 0.6 Hz, 1H), 6.67 (dd, J = 7.8, 1.2 Hz, 1H), 6.56 (m, 1H), 5.94 (s, 1H), 3.91 (s, 1H), 2.39 (s, 1H). ^{13}C NMR (101 MHz, CDCl$_3$) δ 173.2, 159.1, 141.1, 140.3, 138.2, 134.1, 131.7, 128.6, 128.5, 128.1, 127.7, 127.4, 124.0, 111.6, 109.7, 58.6, 56.6, 21.4. HRMS (EI) calcd for $C_{20}H_{19}NOS$ [M]$^+$ 305.1187, found 321.1188.

1-(2-Methyl-(1,1'-biphenylmethyl))-3-methoxyoxypyridin-2-thione (10f). The reaction of **9f** (0.14 g, 0.45 mmol) and Lawesson's reagent (0.11 g, 0.27 mmol) in toluene according to method described for the synthesis of **10a** afforded **10f** (118 mg, 86%) as a yellow solid. ^{1}H NMR (400 MHz, CDCl$_3$) δ 7.42 (dd, J = 6.6, 1.0 Hz, 1H), 7.22 (m, 3H), 6.68 (d, J = 7.3 Hz, 1H), 6.59 (m, 1H), 5.96 (s, 1H), 3.90 (s, 1H), 2.22 (s, 1H). ^{13}C NMR (101 MHz, CDCl$_3$) δ 159.0, 141.5, 140.9, 135.0, 133.6, 131.8, 130.1, 129.5, 129.4, 127.7, 127.2, 125.6, 111.6, 109. 7, 58. 6, 56.6, 20.3. HRMS (EI) calcd for $C_{20}H_{19}NOS$ [M]$^+$ 305.1187, found 321.1189.

1-(4-Dimethylamino-(1,1'-biphenylmethyl))-3-methoxyoxypyridin-2-thione (10g). The reaction of **9g** (0.22 g, 0.67 mmol) and Lawesson's reagent (0.16 g, 0.40 mmol) in toluene according to method described for the synthesis of **10a** afforded **10g** (172 mg, 73%) as a yellow solid. ^{1}H NMR (400 MHz, CDCl$_3$) δ 7.39 (m, 5H), 7.22 (m, 2H), 6.69 (m, 3H), 6.65 (m, 1H), 5.82 (s, 2H), 3.82 (s, 3H), 2.88 (s, 6H). ^{13}C NMR (100 MHz, CDCl$_3$) δ 172.4, 158.7, 149.9, 140. 9, 132.5, 131.8, 128.4, 128.2, 127.3, 126.3, 112.7, 112.0, 110.2, 58.7, 56.3, 40.2. HRMS (EI) calcd for $C_{21}H_{22}N_2OS$ [M]$^+$ 350.1453, found 350.1451.

1-(4-(6-(Dimethylamino)pyridin-3-yl)benzyl))-3-methoxyoxypyridin-2-thione (10h). The reaction of **9h** (0.14 g, 0.42 mmol) and Lawesson's reagent (0.10 g, 0.25 mmol) in toluene according to method described for the synthesis of **10a** afforded **10h** (130 mg, 88%) as a yellow solid. ^{1}H NMR (400 MHz, CDCl$_3$) δ 8.32 (d, J = 2.3 Hz, 1H), 7.56 (dd, J = 8.6, 2.1 Hz, 1H), 7.36 (dd, J = 19.8, 7.3 Hz, 3H), 7.26 (d, J = 8.0 Hz, 2H), 6.61 (d, J = 7.8 Hz, 1H), 6.50 (m, 2H), 5.85 (s, 2H), 3.83 (s, 3H), 3.03 (s, 6H). ^{13}C NMR (100 MHz, CDCl$_3$) δ 172.7, 158.8, 158.3, 145.7, 138.1, 135.3, 133.1, 131.7, 128.5, 126.0, 123.2, 111.6, 109.6, 105.4, 58.4, 56.5, 37.9. HRMS (EI) calcd for $C_{20}H_{21}N_3OS$ [M]$^+$ 351.1405, found 351.1405.

1-(4-(Pyridin-4-yl)benzyl)-3-methoxypyridin-2-thione (10i). The reaction of **9i** (0.13 g, 0.45 mmol) and Lawesson's reagent (0.11 g, 0.27 mmol) in toluene according to method described for the synthesis of **10a** afforded **10i** (104 mg, 76%) as a yellow solid. ^{1}H NMR (400 MHz, CDCl$_3$) δ 8.59 (d, J = 5.9 Hz, 2H), 7.55 (d, J = 8.3 Hz, 2H), 7.39 (m, 5H), 6.67 (dd, J = 7.8, 1.1 Hz, 1H), 6.58 (dd, J = 7.7, 6.7 Hz, 1H), 5.95 (s, 2H), 3.89 (s, 3H). ^{13}C NMR (100 MHz, CDCl$_3$) δ 173.3, 159.2, 150.1, 147.4, 137. 7, 136.2, 131. 8, 128.6, 127.3, 121.4, 111.7, 109. 7, 58.5, 56.7. HRMS (EI) calcd for $C_{18}H_{16}N_2OS$ [M]$^+$ 308.0983, found 308.0975.

Representative Procedure for Deprotection of O-Methyl Group: Synthesis of 11-1-(4-Cyano-(1,1'-biphenylmethyl))-3-hydroxyoxypyridin-2-one (11a). To a solution of **9a** (0.10 g, 0.32 mmol) in dry CH$_2$Cl$_2$ (8 mL) was slowly added 1 M BBr$_3$ (0.35 mL) at −30 °C under argon atmosphere, and the reaction mixture was stirred for 32 h at room temperature. The mixture was again cooled to −30 °C, and then MeOH (5 mL) was slowly added to quench BBr$_3$. Solvent was evaporated off, and the residue was adjusted to pH 7 with aqueous 1 M NaOH and then extracted with CHCl$_3$ (3 × 30 mL). The combined organic layer was dried over Na$_2$SO$_4$, and solvent was evaporated in vacuo. The residue was purified by prep-TLC with CHCl$_3$:acetone:EtOH (10:1:0.2) to give **11a** (89 mg, 94%) as a slightly brownish solid. ^{1}H NMR (400 MHz, DMSO) δ 9.08 (s, 1H), 7.87 (dd, J = 24.8, 7.9 Hz, 4H), 7.71 (d, J = 7.6 Hz, 2H), 7.40 (d, J = 7.7 Hz, 2H), 7.29 (d, J = 6.7 Hz, 1H), 6.70 (d, J = 6.7 Hz, 1H), 6.13 (t, J = 6.8 Hz, 1H), 5.18 (s, 2H). ^{13}C NMR (100 MHz, CDCl$_3$) δ 147.1, 145.1, 139.2, 136.8, 132.9, 129.0, 128.0, 127. 9, 127.1, 119.1, 114.2, 111.4, 107.6, 52.5, 29.9. HRMS (ESI) calcd for $C_{19}H_{15}N_2O_2$ [M + H]$^+$ 303.1128, found 303.1124.

1-(3-Cyano-(1,1′-biphenylmethyl))-3-hydroxyoxypyridin-2-one (11b). The reaction of **9b** (0.05g, 0.15 mmol) with 1 M BBr$_3$ (0.26 mL) in dry CH$_2$Cl$_2$ within 48 h according to the procedure described for the synthesis of **11a** afforded **11b** (44 mg, quantitative) as a brownish solid. ^{1}H NMR (400 MHz, DMSO-d_6) δ 9.08 (s, 1H), 8.11 (s, 1H), 7.98 (d, J = 7.8 Hz, 1H), 7.70 (m, 4H), 7.40 (d, J = 7.7 Hz, 2H), 7.28 (d, J = 6.2 Hz, 1H), 6.70 (d, J = 6.8 Hz, 1H), 6.13 (t, J = 6.7 Hz, 1H), 5.17 (s, 2H). ^{13}C NMR (101 MHz, CDCl$_3$) δ 146. 8, 141.6, 138.6, 136.1, 131.3, 130.8, 130.5, 129.6, 128.7, 127.5, 126.7, 118.7, 113.9, 113.0, 107.3, 52.3. HRMS (EI) calcd for C$_{19}$H$_{14}$N$_2$O$_2$ [M + H]$^+$ 302.1055, found 302.1055.

1-(2-Cyano-(1,1′-biphenylmethyl))-3-hydroxyoxypyridin-2-one (11c). The reaction of **9c** (0.072g, 0.15 mmol) with 1 M BBr$_3$ (0.34 mL) in dry CH$_2$Cl$_2$ within 48 h according to the procedure described for the synthesis of **11a** afforded **11c** (61 mg, 90%) as a brownish solid. ^{1}H NMR (400 MHz, CDCl$_3$) δ 7.75 (d, J = 7.6 Hz, 1H), 7.63 (t, J = 7.7 Hz, 1H), 7.53 (d, J = 7.3 Hz, 1H), 7.43 (m, 2H), 7.12 (m, 1H), 6.86 (dd, J = 28.2, 6.6 Hz, 1H), 6.19 (t, J = 6.1 Hz, 1H), 5.25 (s, 1H). ^{13}C NMR (101 MHz, CDCl$_3$) δ 144. 7, 137.9, 136.4, 133.7, 132.9, 130.0, 129.2, 128.2, 127.7, 118. 6, 111.1, 107.2, 52.1. HRMS (EI) calcd for C$_{19}$H$_{14}$N$_2$O$_2$ [M + H]$^+$ 302.1055, found 302.1053.

1-(4-Methyl-(1,1′-biphenylmethyl))-3-hydroxyoxypyridin-2-one (11d). The reaction of **9d** (0.06 g, 0.20 mmol) with 1 M BBr$_3$ (0.30 mL) in dry CH$_2$Cl$_2$ (5 mL) within 48 h according to the procedure described for the synthesis of **11a** afforded **11d** (57 mg, quantitative) as a brownish solid. ^{1}H NMR (400 MHz, DMSO-d_6) δ 9.07 (s, 1H), 7.57 (m, 2H), 7.50 (d, J = 8.1 Hz, 2H), 7.34 (d, J = 6.8 Hz, 2H), 7.25 (dd, J = 14.8, 7.1 Hz, 3H), 6.69 (d, J = 7.4 Hz, 1H), 6.11 (t, J = 7.1 Hz, 1H), 5.14 (s, 2H), 2.30 (s, 3H). ^{13}C NMR (100 MHz, DMSO-d_6) δ 139.8, 137.3, 137.2, 136.7, 129.9, 128.8, 127.0, 126. 9, 51.7, 21.1. HRMS (EI) calcd for C$_{19}$H$_{17}$NO$_2$ [M]$^+$ 291.1259, found 291.1250.

1-(3-Methyl-(1,1′-biphenylmethyl))-3-hydroxyoxypyridin-2-one (11e). The reaction of **9e** (0.064 g, 0.20 mmol) with 1 M BBr$_3$ (0.30 mL) in dry CH$_2$Cl$_2$ (5 mL) within 48 h according to the procedure described for the synthesis of **11a** afforded **11e** (60 mg, quantitative) as a brownish solid. ^{1}H NMR (400 MHz, CDCl$_3$) δ 7.56 (d, J = 7.5 Hz, 1H), 7.33 (m, 2H), 7.17 (d, J = 7.2 Hz, 1H), 6.85 (dd, J = 22.2, 6.4 Hz, 1H), 6.16 (t, J = 6.5 Hz, 1H), 5.23 (s, 1H), 2.42 (s, 1H). ^{13}C NMR (101 MHz, CDCl$_3$) δ 146.7, 141.2, 140.4, 138.3, 134.7, 128.63, 128.4, 128.2, 127.8, 127. 6, 126.6, 124.1, 113.7, 107.0, 52.1, 21. 5. HRMS (EI) calcd for C$_{19}$H$_{17}$NO$_2$ [M]$^+$ 291.1259, found 291.1263.

1-(2-Methyl-(1,1′-biphenylmethyl))-3-hydroxyoxypyridin-2-one (11f). The reaction of **9f** (0.077 g, 0.25 mmol) with 1 M BBr$_3$ (0.38 mL) in dry CH$_2$Cl$_2$ (5 mL) within 48 h according to the procedure described for the synthesis of **11a** afforded **11f** (65 mg, 90%) as a brownish solid. ^{1}H NMR (400 MHz, CDCl$_3$) δ 7.28 (m, 3H), 6.87 (dd, J = 31.4, 6.8 Hz, 1H), 6.18 (t, J = 6.9 Hz, 1H), 5.27 (d, J = 16.7 Hz, 1H), 2.26 (s, 1H). ^{13}C NMR (101 MHz, CDCl$_3$) δ 146.7, 141.8, 141.1, 135.2, 134.3, 130.3, 129.7, 127.7, 127.4, 126.7, 125.8, 113.6, 107.0, 52.2, 20.4. HRMS (EI) calcd for C$_{19}$H$_{17}$NO$_2$ [M]$^+$ 291.1259, found 291.1260.

1-(4-Dimethylamino-(1,1′-biphenylmethyl))-3-hydroxyoxypyridin-2-one (11g). The reaction of **9g** (0.10 g, 0.30 mmol) with 1 M BBr$_3$ (0.45 mL) in dry CH$_2$Cl$_2$ (8 mL) within 48 h according to the procedure described for the synthesis of **11a** afforded **11g** (84 mg, 87%) as a brownish solid. ^{1}H NMR (400 MHz, DMSO-d_6) δ 9.06 (s, 1H), 7.52 (d, J = 8.0 Hz, 3H), 7.28 (m, 4H), 6.76 (m, 2H), 6.10 (t, J = 5.8 Hz, 1H), 5.12 (s, 2H), 2.90 (s, 6H). ^{13}C NMR (100 MHz, CDCl$_3$) δ 158.7, 150.0, 146.6, 141.1, 135.8, 133.3, 128.8, 128.5, 128.2, 128.1, 128.0, 127.6, 126.6, 113.5, 112.6, 106. 9, 52.1, 40.4. HRMS (EI) calcd for C$_{20}$H$_{20}$N$_2$O$_2$ [M]$^+$ 320.1524, found 320.1512.

1-(4-(6-(Dimethylamino)pyridin-3-yl)benzyl)-3-hydroxyoxypyridin-2-one (11h). The reaction of **9h** (0.10 g, 0.29 mmol) with 1 M BBr$_3$ (0.45 mL) in dry CH$_2$Cl$_2$ (7 mL) within 48 h according to the procedure described for the synthesis of **11a** afforded **11h** (67 mg, 83%) as a brownish solid. ^{1}H NMR (400 MHz, CDCl$_3$) δ 8.40 (s, 1H), 7.66 (d, J = 8.0 Hz, 1H), 7.49 (d, J = 7.7 Hz, 2H), 7.33 (d, J = 7.7 Hz, 2H), 6.84 (dd, J = 27.3, 6.8 Hz, 3H), 6.57 (d, J = 8.7 Hz, 1H), 6.15 (t, J = 7.0 Hz, 1H), 5.20 (s, 2H), 3.12 (s, 6H). ^{13}C NMR (100 MHz, CDCl$_3$) δ 158.5, 146. 7, 145.7, 138.3, 135.8, 133. 9, 132.0, 128.5,

126.8, 126.3, 123.6, 114.2, 107.2, 105.9, 52.1, 38.2. HRMS (EI) calcd for C$_{19}$H$_{19}$N$_3$O$_2$ [M]$^+$ 321.1477, found 321.1479.

1-(4-(Pyridin-4-yl)benzyl)-3-hydroxypyridin-2-one (11i). The reaction of **9i** (0.10 g, 0.34 mmol) with 1 M BBr$_3$ (0.51 mL) in dry CH$_2$Cl$_2$ within 48 h according to the procedure described for the synthesis of **11a** afforded **11i** (79 mg, 83%) as a brownish solid. ^{1}H NMR (400 MHz, CDCl$_3$) δ 8.65 (s, 2H), 7.46 (s, 2H), 7.39 (d, J = 7.9 Hz, 2H), 6.83 (dd, J = 22.5, 7.0 Hz, 2H), 6.16 (t, J = 7.0 Hz, 1H), 5.22 (s, 2H). ^{13}C NMR (100 MHz, CDCl$_3$) δ 150.2, 147.6, 146.8, 138.0, 136.9, 128.7, 127.5, 126.6, 121.6, 113.7, 107.1, 52.2. HRMS (FAB) calcd for C$_{17}$H$_{15}$N$_2$O$_2$ [M + H]$^+$ 279.1133, found 279.1147.

1-(4-Cyano-(1,1′-biphenylmethyl))-3-hydroxyoxypyridin-2-thione (12a). The reaction of **10a** (0.10 g, 0.30 mmol) with 1 M BBr$_3$ (0.33 mL) in dry CH$_2$Cl$_2$ (8 mL) within 48 h according to the procedure described for the synthesis of **11a** afforded **12a** (84 mg, 88%) as a green solid. Retention time 16.58 min (solvent gradient: 40−80% solvent B in 20 min then constant 80% B for 5 min). ^{1}H NMR (400 MHz, DMSO-d_6) δ 7.87 (m, 5H), 7.74 (d, J = 8.1 Hz, 2H), 7.37 (d, J = 8.1 Hz, 2H), 7.04 (m, 1H), 6.90 (d, J = 8.1 Hz, 1H), 5.87 (s, 2H). ^{13}C NMR (100 MHz, CDCl$_3$) δ 164.5, 144.7, 139.2, 134.6, 132.6, 128. 6, 127.7, 127.6, 118.8, 111.2, 61.8, 29.6. HRMS (EI) calcd for C$_{19}$H$_{15}$N$_2$OS [M]$^+$ 318.0827, found 318.0828.

1-(3-Cyano-(1,1′-biphenylmethyl))-3-hydroxyoxypyridin-2-thione (12b). The reaction of **10b** (0.07 g, 0.21 mmol) with 1 M BBr$_3$ (0.32 mL) in dry CH$_2$Cl$_2$ (5 mL) within 48 h according to the procedure described for the synthesis of **11a** afforded **12b** (53 mg, 79%) as a green solid. Retention time 6.93 min (solvent gradient: 70−90% solvent B in 10 min and constant 90% of B for 15 min). ^{1}H NMR (400 MHz, CD$_3$OD) δ 7.89 (m, 2H), 7.65 (m, 5H), 7.44 (d, J = 8.2 Hz, 2H), 7.02 (d, J = 7.7 Hz, 2H), 6.77 (m, 1H), 5.90 (s, 2H). ^{13}C NMR (100 MHz, CD$_3$OD) δ 143.0, 140.0, 132.8, 132.2, 131.7, 131.1, 130.0, 130.0, 129. 9, 128.7, 128.6, 119.8, 113.9, 106.4, 54. 8. HRMS (EI) calcd for C$_{19}$H$_{14}$N$_2$O$_2$ [M + H]$^+$ 318.0827, found 318.0827

1-(2-Cyano-(1,1′-biphenylmethyl))-3-hydroxyoxypyridin-2-thione (12c). The reaction of **10c** (0.042 g, 0.21 mmol) with 1 M BBr$_3$ (0.19 mL) in dry CH$_2$Cl$_2$ (5 mL) within 48 h according to the procedure described for the synthesis of **11a** afforded **12c** (31 mg, 78%) as a green solid. Retention time 12.37 min (solvent gradient: 40−80% solvent B in 20 min then constant 80% B for 5 min). ^{1}H NMR (400 MHz, CD$_3$OD) δ 7.77 (dd, J = 7.7, 0.9 Hz, 1H), 7.67 (m, 2H), 7.48 (m, 4H), 7.01 (d, J = 13.1 Hz, 1H), 6.70 (m, 1H), 5.90 (s, 1H). ^{13}C NMR (101 MHz, CD$_3$OD) δ 145.3, 138.9, 134.4, 133.9, 130.8, 129.9, 128.9, 128.6, 119.2, 115.1, 111.4. HRMS (EI) calcd for C$_{19}$H$_{14}$N$_2$O$_2$ [M + H]$^+$ 318.0821, found 318.0827

1-(4-Methyl-(1,1′-biphenylmethyl))-3-hydroxyoxypyridin-2-thi-one (12d). The reaction of **10d** (0.06 g, 0.20 mmol) with 1 M BBr$_3$ (0.30 mL) in dry CH$_2$Cl$_2$ (5 mL) within 48 h according to the procedure described for the synthesis of **11a** afforded **12d** (45 mg, 73%) as a green solid. Retention time 11.53 min (solvent gradient: 70−90% solvent B in 10 min and constant 90% of B for 15 min). ^{1}H NMR (400 MHz, CD$_3$OD) δ 7.70 (d, J = 1.1 Hz, 1H), 7.63 (d, J = 6.3 Hz, 1H), 7.55 (d, J = 8.2 Hz, 2H), 7.40 (m, 3H), 7.21 (d, J = 8.1 Hz, 2H), 7.03 (dd, J = 14.9, 7.8 Hz, 2H), 6.75 (t, J = 7.0 Hz, 1H), 5.87 (s, 2H), 2.35 (s, 3H). ^{13}C NMR (100 MHz, CD3OD) δ 141.4, 137.15, 133.66, 131.83, 129.27, 128.43, 127.05, 126.59, 113.79, 112.26, 59.63, 20.32. HRMS (EI) calcd for C$_{19}$H$_{17}$NOS [M]$^+$ 307.1031, found 307.1022.

1-(3-Methyl-(1,1′-biphenylmethyl))-3-hydroxyoxypyridin-2-thi-one (12e). The reaction of **10e** (0.08 g, 0.20 mmol) with 1 M BBr$_3$ (0.36 mL) in dry CH$_2$Cl$_2$ (5 mL) within 48 h according to the procedure described for the synthesis of **11a** afforded **12e** (51 mg, 70%) as a green solid. Retention time 10.52 min (solvent gradient: 70−90% solvent B in 10 min and constant 90% of B for 15 min). ^{1}H NMR (400 MHz, CD$_3$OD) δ 7.53 (m, 1H), 7.30 (m, 2H), 7.12 (d, J = 7.2 Hz, 1H), 6.97 (m, 1H), 6.68 (m, 1H), 5.81 (s, 1H), 2.36 (s, 1H). ^{13}C NMR (101 MHz, CD$_3$OD) δ 141.5, 140.2, 138.3, 128.6, 128.5, 128.2, 127.7, 127.5, 124.0, 21.2. HRMS (EI) calcd for C$_{19}$H$_{17}$NOS [M]$^+$ 307.1031, found 307.1031.

1-(2-Methyl-(1,1′-biphenylmethyl))-3-hydroxyoxypyridin-2-thi-one (12f). The reaction of **10f** (0.08 g, 0.20 mmol) with 1 M BBr$_3$

(0.36 mL) in dry CH_2Cl_2 (5 mL) within 48 h according to the procedure described for the synthesis of **11a** afforded **12f** (49 mg, 67%) as a green solid. Retention time 17.67 min (solvent gradient: 40−80% solvent B in 20 min then constant 80% B for 5 min). ^{1}H NMR (400 MHz, CD_3OD) δ 7.54 (m, 1H), 7.19 (m, 3H), 6.98 (m, 1H), 6.70 (m, 1H), 5.83 (s, 1H), 2.19 (s, 1H). ^{13}C NMR (100 MHz, CD_3OD) δ 142.1, 141.0, 135.1, 130.2, 129.6, 129.5, 127.8, 127.3, 125.7, 20.0. HRMS (EI) calcd for $C_{19}H_{17}NOS$ $[M]^+$ 307.1031, found 307.1034.

1-(4-Dimethylamino-(1,1′-biphenylmethyl))-3-hydroxyoxypyridin-2-thione (12g). The reaction of **10g** (0.11 g, 0.33 mmol) with 1 M BBr_3 (0.39 mL) in dry CH_2Cl_2 (5 mL) within 48 h according to the procedure described for the synthesis of **11a** afforded **12g** (68 mg, 62%) as a green solid. Retention time 10.42 min (solvent gradient: 70−90% solvent B in 10 min and constant 90% of B for 15 min). ^{1}H NMR (400 MHz, $CDCl_3$) δ 8.57 (d, J = 8.5 Hz, 1H), 7.53 (d, J = 8.2 Hz, 2H), 7.46 (m, 2H), 7.33 (d, J = 8.0 Hz, 3H), 6.97 (d, J = 6.8 Hz, 1H), 6.77 (d, J = 8.8 Hz, 2H), 6.62 (m, 1H), 5.79 (s, 2H), 2.98 (s, 6H). ^{13}C NMR (100 MHz, $CDCl_3$) δ 169.7, 155.1, 150.1, 141.5, 131.9, 130.8, 129.0, 128.8, 128.0, 127.6, 126.7, 113.6, 112.6, 111.9, 60.1, 40. 5. HRMS (EI) calcd for $C_{20}H_{20}N_2OS$ $[M]^+$ 336.1296, found 336.1295.

1-(4-(6-(Dimethylamino)pyridin-3-yl)benzyl))-3-hydroxyoxypyridin-2-thione (12h). The reaction of **10h** (0.064 g, 0.18 mmol) with 1 M BBr_3 (0.27 mL) in dry CH_2Cl_2 (5 mL) within 48 h according to the procedure described for the synthesis of **11a** afforded **12h** (48 mg, 79%) as a green solid. Retention time 27.43 min (solvent gradient: 40−80% solvent B in 20 min then constant 80% B for 15 min). ^{1}H NMR (400 MHz, $CDCl_3$) δ 8.30 (s, 1H), 7.70 (d, J = 8.9 Hz, 1H), 7.46 (s, 2H), 7.31 (t, J = 7.6 Hz, 3H), 6.98 (d, J = 7.8 Hz, 1H), 6.67 (m, 2H), 5.75 (s, 2H), 3.11 (s, 8H). ^{13}C NMR (100 MHz, $CDCl_3$) δ 157.0, 143. 5, 142.2, 137.7, 137.0, 132.8, 128.8, 127. 6, 126.4, 123.7, 114.4, 107.0, 38.5, 29.5. HRMS (EI) calcd for $C_{19}H_{19}N_3OS$ $[M]^+$ 337.1249, found 337.1251.

1-(4-(Pyridin-4-yl)benzyl)-3-hydroxypyridin-2-thione (12i). The reaction of **10i** (0.08 g, 0.25 mmol) with 1 M BBr_3 (0.38 mL) in dry CH_2Cl_2 (5 mL) within 48 h according to the procedure described for the synthesis of **11a** afforded **12i** (65 mg, 88%) as a green solid. Retention time 19.37 min (solvent gradient: 40−80% solvent B in 20 min then constant 80% B for 10 min). ^{1}H NMR (400 MHz, $CDCl_3$) δ 8.65 (d, J = 5.3 Hz, 2H), 8.55 (s, 1H), 7.62 (d, J = 8.0 Hz, 2H), 7.42 (m, 5H), 6.99 (d, J = 7.5 Hz, 1H), 6.67 (t, J = 7.0 Hz, 1H), 5.85 (s, 2H). ^{13}C NMR (100 MHz, $CDCl_3$) δ 170.1, 155.3, 150.3, 147.4, 138.2, 135.5, 130.9, 128.8, 127.6, 121.5, 113.7, 111.9, 59.9. HRMS (EI) calcd for $C_{17}H_{14}N_2OS$ $[M]^+$ 294.0827, found 294.0823.

1-Propargyl-3-methoxypyridin-2-one (13). To a stirring solution of 3-methoxy-2-pyridinone (1.00 g, 8.00 mmol) in DMF (25 mL) was added propargyl bromide (80 wt % solution in toluene, 1.5 equiv) and K_2CO_3 (3.313 g, 24 mmol). The reaction mixture was heated overnight at 100 °C and allowed to cool to room temperature. The reaction was partitioned between EtOAc (120 mL) and water (100 mL). The organic layer was separated, washed repeatedly with water (7 × 100 mL) and brine (60 mL) and dried on Na_2SO_4. Solvent was evaporated in vacuo, and the dark-brown crude was purified by column chromatography using a gradient of 0−20% acetone in CH_2Cl_2 to give **13** (0.79 g, 60%) as a brownish solid. ^{1}H NMR ($CDCl_3$, 400 MHz) δ 2.36 (1H, t, J = 2.8), 3.67 (3H, m), 4.66 (1H, d, J = 2.8), 6.05 (1H, t, J = 7.2), 6.50 (1H, dd, J = 1.6, 7.2), 7.11 (1H, dd, J = 1.6, 6.8). ^{13}C NMR ($CDCl_3$, 100 MHz) δ 37.2, 55.5, 74.6, 77.3, 104.8, 112.0, 126.3, 149.4, 157.1. HRMS (EI) calcd for $C_9H_9NO_2$ $[M]^+$ 163.0633, found 163.0636

1-Phenyltriazolylmethyl-3-methoxypyridin-2-one (14a). Compound **13** (0.32 g, 1.95 mmol) and phenylazide (0.35 g, 2.93 mmol) were dissolved in anhydrous THF (10 mL) and stirred under argon at room temperature. Copper(I) iodide (0.01 g, 0.07 mmol) and Hunig's base (0.1 mL) were added to the reaction mixture, and stirring continued for 4 h. The reaction mixture was diluted with CH_2Cl_2 (40 mL) and washed with 1:4 NH_4OH/saturated NH_4Cl (3 × 30 mL) and saturated NH_4Cl (30 mL). The organic layer was dried over Na_2SO_4 and concentrated in vacuo. The crude product was triturated with hexanes to give **14a** (510 mg, 92%) as a white solid. ^{1}H NMR ($CDCl_3$,

400 MHz) δ 3.58 (3H, s), 5.11 (2H, s), 5.93 (1H, t, J = 7.6), 6.42 (1H, d, J = 7.2), 7.07 (1H, d, J = 6.4), 7.16−7.20 (1H, m), 7.26 (2H, t, J = 7.6), 7.49 (2H, d, J = 8.0). ^{13}C NMR ($CDCl_3$, 100 MHz) δ 44.2, 55.2, 104.7, 112.0, 119.7, 121.8, 127.9, 128.1, 129.0, 136.2, 142.8, 149.3, 157.2. HRMS (EI) calcd for $C_{15}H_{14}N_4O_2$ $[M]^+$ 282.1117, found 282.1115.

1-(4-Dimethylamino)phenylltriazolylmethyl-3-methoxypyridin-2-one (14b). The reaction of 4-azido-N,N-dimethylaniline (0.09 g, 0.61 mmol) and **13** (0.10 g, 0.61 mmol) within 4 h as described for the synthesis of **14a** gave compound **14b** (0.13 g, 68%) as a white solid. ^{1}H NMR (400 MHz, $CDCl_3$) δ 8.04 (s, 1H), 7.41 (m, 2H), 7.15 (dd, J = 6.9, 1.7 Hz, 1H), 6.62 (m, 2H), 6.51 (dd, J = 7.5, 1.6 Hz, 1H), 6.03 (m, 1H), 5.19 (s, 2H), 3.70 (s, 3H), 2.89 (s, 6H). ^{13}C NMR (100 MHz, $CDCl_3$) δ 157.5, 150.2, 149.7, 142.6, 128.2, 126.2, 121.9, 121.4, 112.2, 111.8, 104.9, 55.6, 44.5, 40.1. HRMS (EI) calcd for $C_{17}H_{19}N_5O_2$ $[M]^+$ 325.1539, found 325.1544.

1-Phenyltriazolylmethyl-3-hydroxypyridin-2-one (15a). The reaction of **14a** (0.21 g, 0.75 mmol) and 1 M BBr_3 in CH_2Cl_2 (1.5 equiv) withing 48 h as described for the synthesis of **11a** gave compound **15a** (0.123 g, 61%) as a brown solid. ^{1}H NMR (DMSO-d_6, 400 MHz) δ 5.27 (2H, s), 6.13 (1H, t, J = 6.4), 6.67 (1H, d, J = 7.2), 7.30 (1H, d, J = 5.6), 7.45−7.49 (1H, m), 7.57 (2H, t, J = 7.6), 7.87 (2H, d, J = 8.0), 8.73 (1H, s), 9.08 (1H, s). ^{13}C NMR (101 MHz, $CDCl_3$) δ 136.6, 129.6, 128.9, 122.3, 120.6, 108.0, 29.3. HRMS (EI) calcd for $C_{14}H_{12}N_4O_2$ $[M]^+$ 268.0960, found 268.0967.

1-(4-Dimethylamino)phenylltriazolylmethyl-3-hydroxypyridin-2-one (15b). The reaction of **14b** (0.045 g, 0.14 mmol) and 1 M BBr_3 in CH_2Cl_2 (0.22 mL, 1.5 equiv) withing 48 h as described for the synthesis of **11a** gave compound **15b** (0.033 g, 77%) as a brown solid. ^{1}H NMR (400 MHz, $CDCl_3$) δ 8.08 (s, 1H), 7.48 (dd, J = 19.9, 8.4 Hz, 2H), 7.18 (d, J = 6.7 Hz, 1H), 6.69 (ddd, J = 25.8, 24.8, 7.5 Hz, 4H), 6.16 (t, J = 6.9 Hz, 1H), 5.31 (s, 2H), 2.98 (m, 6H). ^{13}C NMR (101 MHz, $CDCl_3$) δ 158.4, 150.5, 146.7, 142.5, 127.1, 126.4, 122.1, 121.9, 121.8, 112.1, 107.1, 44.7, 40.3. HRMS (EI) calcd for $C_{16}H_{17}N_5O_2$ $[M]^+$ 311.1382, found 311.1386.

1-Phenyltriazolylmethyl-3-methoxypyridin-2-thione (16a). The reaction of **14a** (0.30 g, 1.04 mmol) and Lawesson's reagent (0.25 g, 0.62 mmol) in toluene (15 mL) within 12 h as described for the synthesis of **10a** gave compound **16a** (0.29 g, 94%) as a yellow solid. ^{1}H NMR ($CDCl_3$, 400 MHz) δ 3.90 (3H, s), 6.04 (2H, s), 6.62−6.68 (2H, m), 7.38−7.42 (1H, m), 7.48 (2H, t, J = 7.2), 7.68 (2H, d, J = 8.0), 7.82 (1H, d, J = 4.8), 8.53 (1H, s). ^{13}C NMR ($CDCl_3$, 100 MHz) δ 50.9, 56.4, 110.0, 112.0, 120.2, 122.4, 128.5, 129.3, 132.2, 136.4, 141.9, 158.7, 171.5. HRMS (EI) calcd for $C_{15}H_{14}N_4O_2$ $[M]^+$ 282.1117, found 282.1115. HRMS (EI) calcd for $C_{15}H_{14}N_4OS$ $[M]^+$ 298.0888, found 298.0888.

1-(4-Dimethylamino)phenylltriazolylmethyl-3-methoxypyridin-2-thione (16b). The reaction of **14b** (0.08 g, 0.25 mmol) and Lawesson's reagent (0.06 g, 0.15 mmol) in toluene (8 mL) within 12 h as described for the synthesis of **10a** gave compound **16b** (0.07 g, 84%) as a yellow solid. ^{1}H NMR (400 MHz, cdcl$_3$) δ 8.36 (s, 1H), 7.81 (dd, J = 6.4, 1.5 Hz, 1H), 7.46 (m, 2H), 6.66 (m, 4H), 6.01 (s, 2H), 3.87 (s, 3H), 2.97 (s, 6H). ^{13}C NMR (100 MHz, $CDCl_3$) δ 171.8, 158.9, 150.4, 141.5, 132.4, 126.3, 122.5, 121.8, 112.1, 112.0, 110.1, 56.7, 51.2, 40.3. HRMS (EI) calcd for $C_{17}H_{19}N_5OS$ $[M]^+$ 314.1310, found 314.1304.

1-Phenyltriazolylmethyl-3-hydroxypyridin-2-thione (17a). The reaction of **16a** (0.28 g, 0.93 mmol) and 1 M BBr_3 in CH_2Cl_2 (1.5 equiv) within 48 h as described for the synthesis of **11a** gave compound **17a** (0.18 g, 67%) as a green solid. Retention time 8.63 min (solvent gradient: 40−80% solvent B in 20 min then constant 80% B for 5 min). ^{1}H NMR (400 MHz, $CDCl_3$) δ 8.43 (d, J = 16.6 Hz, 1H), 8.39 (s, 1H), 7.79 (dd, J = 6.6, 1.3 Hz, 1H), 7.69 (m, 2H), 7.46 (m, 3H), 6.97 (dd, J = 7.7, 1.2 Hz, 1H), 6.69 (dd, J = 7.6, 6.8 Hz, 1H), 5.94 (s, 2H). ^{13}C NMR (100 MHz, CDC_3) δ 168.6, 155.1, 141.6, 136.7, 131.7, 129.7, 129.0, 122.6, 120.6, 114.0, 112.5, 77.3, 77.0, 76. 7, 52.1. HRMS (EI) calcd for $C_{14}H_{12}N_4OS$ $[M]^+$ 284.0730, found 284.0732.

1-(4-Dimethylamino)phenylltriazolylmethyl-3-hydroxypyridin-2-thione (17b). The reaction of **16b** (0.07 g, 0.21 mmol) and 1 M BBr_3

in CH_2Cl_2 (0.64 mL, 1.5 equiv) within 48 h as described for the synthesis of **11a** gave compound **17b** (0.03 g, 48%) as a green solid. Retention time 8.43 min (solvent gradient: 40−80% solvent B in 20 min then constant 80% B for 5 min). ^{1}H NMR (400 MHz, CDCl$_3$) δ 8.42 (s, 1H), 8.29 (d, J = 11.5 Hz, 1H), 7.79 (d, J = 6.4 Hz, 1H), 7.50 (m, 2H), 6.98 (dd, J = 36.5, 28.9 Hz, 2H), 6.72 (m, 3H), 5.94 (s, 2H), 3.01 (d, J = 2.7 Hz, 6H). ^{13}C NMR (100 MHz, CDCl$_3$) δ 155.1, 150.7, 141.1, 131.7, 127.7, 126.3, 122. S, 122.0, 114.0, 112.5, 112.2, 52.2, 40.4. HRMS (EI) calcd for $C_{16}H_{17}N_5OS$ [M]$^+$ 327.1154, found 327.1154.

ASSOCIATED CONTENT

Ⓢ Supporting Information

^{1}H NMR and ^{13}C NMR spectral information, solubility data and molecular modeling outputs. This material is available free of charge via the Internet at http://pubs.acs.org.

AUTHOR INFORMATION

Corresponding Author

*For M.M.: phone, 847-467-0472; fax, 847-467-3057; E-mail, milan.mrksich@northwestern.edu. For A.K.O.: phone, 404-894-4047; fax, 404-894-2291; E-mail, aoyelere@gatech.edu.

Author Contributions

||These authors contributed equally to the manuscript.

Notes

The authors declare no competing financial interest.

ACKNOWLEDGMENTS

ABBREVIATIONS USED

HDAC, histone deacetylase; HAT, histone acetyltransferase; HDACi, histone deacetylase inhibitors; ZBG, zinc binding group; SAHA, suberoylanilide hydroxamic acid; TSA, trichostatin A; 3HPT, 3-hydroxypyridin-2-thione; MMP, matrix metalloproteins

REFERENCES

(1) Esteller, M. Cancer epigenomics: DNA methylomes and histone-modification maps. *Nature Rev. Genet.* **2007**, *8* (4), 286−298.

(2) Kornberg, R. D.; Lorch, Y. Twenty-Five Years of the Nucleosome, Fundamental Particle of the Eukaryote Chromosome. *Cell* **1999**, *98* (3), 285−294.

(3) Grunstein, M. Histone acetylation in chromatin structure and transcription. *Nature* **1997**, *389* (6649), 349−352.

(4) Gryder, B. E.; Sodji, Q. H.; Oyelere, A. K. Targeted cancer therapy: giving histone deacetylase inhibitors all they need to succeed. *Future Med. Chem.* **2012**, *4* (4), 505−524.

(5) Glozak, M. A.; Sengupta, N.; Zhang, X.; Seto, E. Acetylation and deacetylation of non-histone proteins. *Gene* **2005**, *363* (0), 15−23.

(6) Weichert, W. HDAC expression and clinical prognosis in human malignancies. *Cancer Lett.* **2009**, *280* (2), 168−176.

(7) Cardinale, J. P.; Sriramula, S.; Pariaut, R.; Guggilam, A.; Mariappan, N.; Elks, C. M.; Francis, J. HDAC Inhibition Attenuates Inflammatory, Hypertrophic, and Hypertensive Responses in Spontaneously Hypertensive Rats. *Hypertension* **2010**, *56* (3), 437−444.

(8) Patil, V.; Guerrant, W.; Chen, P. C.; Gryder, B.; Benicewicz, D. B.; Khan, S. I.; Tekwani, B. L.; Oyelere, A. K. Antimalarial and antileishmanial activities of histone deacetylase inhibitors with triazole-linked cap group. *Bioorg. Med. Chem.* **2010**, *18* (1), 415−425.

(9) Rotili, D.; Simonetti, G.; Savarino, A.; Palamara, A. T.; Migliaccio, A. R.; Mai, A. Non-cancer uses of histone deacetylase inhibitors: effects on infectious diseases and beta-hemoglobinopathies. *Curr. Top. Med. Chem.* **2009**, *9* (3), 272−291.

(10) Chuang, D.-M.; Leng, Y.; Marinova, Z.; Kim, H.-J.; Chiu, C.-T. Multiple roles of HDAC inhibition in neurodegenerative conditions. *Trends Neurosci.* **2009**, *32* (11), 591−601.

(11) Miller, T. A.; Witter, D. J.; Belvedere, S. Histone Deacetylase Inhibitors. *J. Med. Chem.* **2003**, *46* (24), 5097−5116.

(12) Finnin, M. S.; Donigian, J. R.; Cohen, A.; Richon, V. M.; Rifkind, R. A.; Marks, P. A.; Breslow, R.; Pavletich, N. P. Structures of a histone deacetylase homologue bound to the TSA and SAHA inhibitors. *Nature* **1999**, *401* (6749), 188−193.

(13) Jerry, W. S.; Nina, C. G.; Arco, Y. J. The Design, Structure, and Clinical Update of Small Molecular Weight Matrix Metalloproteinase Inhibitors. *Curr. Med. Chem.* **2004**, *11* (22), 2911−2977.

(14) Whittaker, M.; Floyd, C. D.; Brown, P.; Gearing, A. J. H. Design and Therapeutic Application of Matrix Metalloproteinase Inhibitors. *Chem. Rev.* **1999**, *99* (9), 2735−2776.

(15) Reiter, L. A.; Robinson, R. P.; McClure, K. F.; Jones, C. S.; Reese, M. R.; Mitchell, P. G.; Otterness, I. G.; Bliven, M. L.; Liras, J.; Cortina, S. R.; Donahue, K. M.; Eskra, J. D.; Griffiths, R. J.; Lame, M. E.; Lopez-Anaya, A.; Martinelli, G. J.; McGahee, S. M.; Yocum, S. A.; Lopresti-Morrow, L. L.; Tobiassen, L. M.; Vaughn-Bowser, M. L. Pyran-containing sulfonamide hydroxamic acids: potent MMP inhibitors that spare MMP-1. *Bioorg. Med. Chem. Lett.* **2004**, *14* (13), 3389−3395.

(16) Frey, R. R.; Wada, C. K.; Garland, R. B.; Curtin, M. L.; Michaelides, M. R.; Li, J.; Pease, L. J.; Glaser, K. B.; Marcotte, P. A.; Bouska, J. J.; Murphy, S. S.; Davidsen, S. K. Trifluoromethyl ketones as inhibitors of histone deacetylase. *Bioorg. Med. Chem. Lett.* **2002**, *12* (23), 3443−3447.

(17) Coussens, L. M.; Fingleton, B.; Matrisian, L. M. Matrix Metalloproteinase Inhibitors and Cancer—Trials and Tribulations. *Science* **2002**, *295* (5564), 2387−2392.

(18) Farkas, E.; Katz, Y.; Bhusare, S.; Reich, R.; Röschenthaler, G.-V.; Königsmann, M.; Breuer, E. Carbamoylphosphonate-based matrix metalloproteinase inhibitor metal complexes: solution studies and stability constants. Towards a zinc-selective binding group. *J. Biol. Inorg. Chem.* **2004**, *9* (3), 307−315.

(19) O'Brien, E. C.; Farkas, E.; Gil, M. J.; Fitzgerald, D.; Castineras, A.; Nolan, K. B. Metal complexes of salicylhydroxamic acid (H2Sha), anthranilic hydroxamic acid and benzohydroxamic acid. Crystal and molecular structure of [Cu(phen)2(Cl)]Cl·H2Sha, a model for a peroxidase-inhibitor complex. *J. Inorg. Biochem.* **2000**, *79* (1−4), 47−51.

(20) Oyelere, A. K.; Chen, P. C.; Guerrant, W.; Mwakwari, S. C.; Hood, R.; Zhang, Y.; Fan, Y. Non-Peptide Macrocyclic Histone Deacetylase Inhibitors. *J. Med. Chem.* **2008**, *52* (2), 456−468.

(21) Butler, K. V.; Kalin, J.; Brochier, C.; Vistoli, G.; Langley, B.; Kozikowski, A. P. Rational Design and Simple Chemistry Yield a Superior, Neuroprotective HDAC6 Inhibitor, Tubastatin A. *J. Am. Chem. Soc.* **2010**, *132* (31), 10842−10846.

(22) Suzuki, T.; Miyata, N. Non-hydroxamate Histone Deacetylase Inhibitors. *Curr. Med. Chem.* **2005**, *12* (24), 2867−2880.

(23) Khan, N.; Jeffers, M.; Kumar, S.; Hackett, C.; Boldog, F.; Khramtsov, N.; Qian, X. Z.; Mills, E.; Berghs, S. C.; Carey, N.; Finn, P. W.; Collins, L. S.; Tumber, A.; Ritchie, J. W.; Jensen, P. B.; Lichenstein, H. S.; Sehested, M. Determination of the class and isoform selectivity of small-molecule histone deacetylase inhibitors. *Biochem. J.* **2008**, *409*, 581−589.

(24) Saito, A.; Yamashita, T.; Mariko, Y.; Nosaka, Y.; Tsuchiya, K.; Ando, T.; Suzuki, T.; Tsuruo, T.; Nakanishi, O. A synthetic inhibitor of histone deacetylase, MS-27-275, with marked in vivo antitumor activity against human tumors. *Proc. Natl. Acad. Sci. U. S. A.* **1999**, *96* (8), 4592−4597.

(25) Monneret, C. Histone deacetylase inhibitors. *Eur. J. Med. Chem.* **2005**, *40* (1), 1−13.

(26) Jacobsen, F. E.; Lewis, J. A.; Cohen, S. M. The Design of Inhibitors for Medicinally Relevant Metalloproteins. *ChemMedChem* **2007**, *2* (2), 152−171.

(27) Puerta, D. T.; Lewis, J. A.; Cohen, S. M. New Beginnings for Matrix Metalloproteinase Inhibitors: Identification of High-Affinity Zinc-Binding Groups. *J. Am. Chem. Soc.* **2004**, *126* (27), 8388−8389.

(28) Lewis, J. A.; Tran, B. L.; Puerta, D. T.; Rumberger, E. M.; Hendrickson, D. N.; Cohen, S. M. Synthesis, structure and spectroscopy of new thiopyrone and hydroxypyridinethione transition-metal complexes. *Dalton Trans.* **2005**, *15*, 2588−2596.

(29) Somoza, J. R.; Skene, R. J.; Katz, B. A.; Mol, C.; Ho, J. D.; Jennings, A. J.; Luong, C.; Arvai, A.; Buggy, J. J.; Chi, E.; Tang, J.; Sang, B.-C.; Verner, E.; Wynands, R.; Leahy, E. M.; Dougan, D. R.; Snell, G.; Navre, M.; Knuth, M. W.; Swanson, R. V.; McRee, D. E.; Tari, L. W. Structural Snapshots of Human HDAC8 Provide Insights into the Class I Histone Deacetylases. *Structure* **2004**, *12* (7), 1325−1334.

(30) Mwakwari, S. C.; Guerrant, W.; Patil, V.; Khan, S. I.; Tekwani, B. L.; Gurard-Levin, Z. A.; Mrksich, M.; Oyelere, A. K. Non-Peptide Macrocyclic Histone Deacetylase Inhibitors Derived from Tricyclic Ketolide Skeleton. *J. Med. Chem.* **2010**, *53* (16), 6100−6111.

(31) Morris, G. M.; Goodsell, D. S.; Halliday, R. S.; Huey, R.; Hart, W. E.; Belew, R. K.; Olson, A. J. Automated docking using a Lamarckian genetic algorithm and an empirical binding free energy function. *J. Comput. Chem.* **1998**, *19* (14), 1639−1662.

(32) Davies, J. S.; Smith, K.; Turner, J. Novel heterocyclic systems, Part 4: A simple, convenient synthesis of 3-hydroxypyridine-2-thione, and the preparation of two novel tricyclic betaines. *Tetrahedron Lett.* **1980**, *21* (22), 2191−2194.

(33) Gurard-Levin, Z. A.; Mrksich, M. The Activity of HDAC8 Depends on Local and Distal Sequences of Its Peptide Substrates. *Biochemistry* **2008**, *47* (23), 6242−6250.

(34) Gurard-Levin, Z. A.; Scholle, M. D.; Eisenberg, A. H.; Mrksich, M. High-Throughput Screening of Small Molecule Libraries using SAMDI Mass Spectrometry. *ACS Comb. Sci.* **2011**, *13* (4), 347−350.

(35) Srogl, J.; Liu, W.; Marshall, D.; Liebeskind, L. S. Bio-organometallic Organosulfur Chemistry. Transition Metal-Catalyzed Cross-Coupling Using Coenzyme M or Thioglycolic Acid as the Leaving Group. *J. Am. Chem. Soc.* **1999**, *121* (40), 9449−9450.

(36) Miyaura, N.; Yamada, K.; Suzuki, A. A new stereospecific cross-coupling by the palladium-catalyzed reaction of 1-alkenylboranes with 1-alkenyl or 1-alkynyl halides. *Tetrahedron Lett.* **1979**, *20* (36), 3437−3440.

(37) Egan, W. J.; Lauri, G. Prediction of intestinal permeability. *Adv. Drug Delivery Rev.* **2002**, *54* (3), 273−289.

(38) Guerrant, W.; Patil, V.; Canzoneri, J. C.; Oyelere, A. K. Dual Targeting of Histone Deacetylase and Topoisomerase II with Novel Bifunctional Inhibitors. *J. Med. Chem.* **2012**, *55* (4), 1465−1477.

(39) Namdar, M.; Perez, G.; Ngo, L.; Marks, P. A. Selective inhibition of histone deacetylase 6 (HDAC6) induces DNA damage and sensitizes transformed cells to anticancer agents. *Proc. Natl. Acad. Sci. U. S. A.* **2010**, *107* (46), 20003−20008.

(40) Yamaki, H.; Nakajima, M.; Shimotohno, K. W.; Tanaka, N. Molecular basis for the actions of Hsp90 inhibitors and cancer therapy. *J. Antibiot.* **2011**, *64* (9), 635−644.

(41) Balasubramanian, S.; Ramos, J.; Luo, W.; Sirisawad, M.; Verner, E.; Buggy, J. J. A novel histone deacetylase 8 (HDAC8)-specific inhibitor PCI-34051 induces apoptosis in T-cell lymphomas. *Leukemia* **2008**, *22* (5), 1026−1034.

(42) Lipinski, C. A.; Lombardo, F.; Dominy, B. W.; Feeney, P. J. Experimental and computational approaches to estimate solubility and permeability in drug discovery and development settings. *Adv. Drug Delivery Rev.* **1997**, *23* (1−3), 3−25.

(43) Kerns, E. H.; Di, L.; Carter, G. T. In Vitro Solubility Assays in Drug Discovery. *Curr. Drug Metab.* **2008**, *9* (9), 879−885.

(44) Kulp, S. K.; Chen, C.-S.; Wang, D.-S.; Chen, C.-Y.; Chen, C.-S. Antitumor Effects of a Novel Phenylbutyrate-Based Histone Deacetylase Inhibitor, (S)-HDAC-42, in Prostate Cancer. *Clin. Cancer Res.* **2006**, *12* (17), 5199−5206.

(45) Chakraborty, A.; Dey, S.; Sawoo, S.; Adarsh, N. N.; Sarkar, A. Regioselective 1,3-Dipolar Cycloaddition Reaction of Azides with Alkoxy Alkynyl Fischer Carbene Complexes. *Organometallics* **2010**, *29* (23), 6619−6622.

(46) Andersen, J.; Bolvig, S.; Liang, X. Efficient One-Pot Synthesis of 1-Aryl 1,2,3-Triazoles from Aryl Halides and Terminal Alkynes in the Presence of Sodium Azide. *Synlett* **2005**, *2005* (EFirst), 2941−2947.